JCI The Journal of Clinical Investigation

17β-estradiol and estrogen receptor-α protect right ventricular function in pulmonary hypertension via BMPR2 and apelin

Andrea L. Frump, … , Sebastien Bonnet, Tim Lahm

J Clin Invest. 2021. https://doi.org/10.1172/JCI129433.

Research In-Press Preview Pulmonology Vascular biology

Graphical abstract

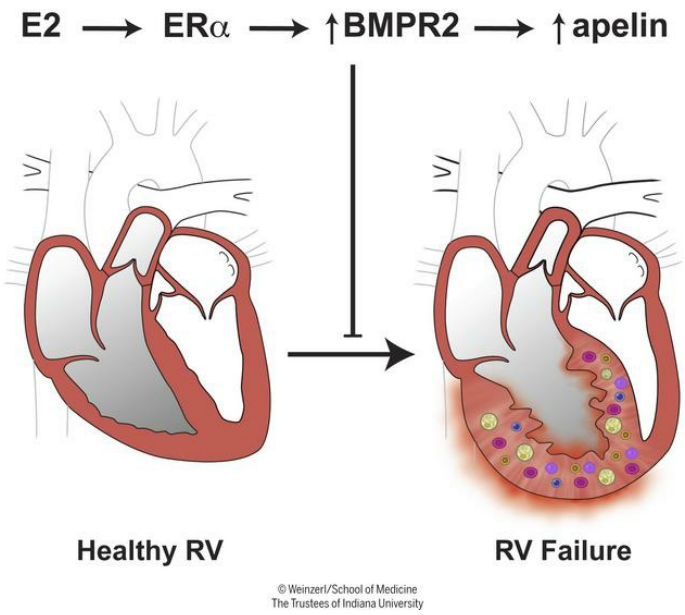

Find the latest version:

https://jci.me/129433/pdf

17β-estradiol and estrogen receptor-α protect right ventricular function in pulmonary hypertension via BMPR2 and apelin

Andrea L. Frump[1], Marjorie Albrecht[1], Bakhtiyor Yakubov[1], Sandra Breuils-Bonnet[2], Valérie Nadeau[2], Eve Tremblay[2], Francois Potus[2], Junichi Omura[2], Todd Cook[1], Amanda Fisher[1], Brooke Rodriguez[1], R. Dale Brown[3], Kurt R. Stenmark[3], C. Dustin Rubinstein[4], Kathy Krentz[4], Diana M. Tabima[5], Rongbo Li[6*], Xin Sun[6*], Naomi C. Chesler[5], Steeve Provencher[2], Sebastien Bonnet[2], Tim Lahm[1,7,8]

[1]Department of Medicine; Division of Pulmonary, Critical Care, Sleep and Occupational Medicine, Indiana University School of Medicine, Indianapolis, IN; [2]Pulmonary hypertension research group, Institute Universitaire de Cardiologie et de Pneumologie de Québec – Université Laval, Quebec City, Quebec, Canada; [3]Department of Pediatrics, University of Colorado-Denver, Aurora, CO; [4]Genome Editing and Animal Models Core, University of Wisconsin Biotechnology Center; [5]Biomedical Engineering, University of Wisconsin-Madison, Madison, WI; [6]Genetics, University of Wisconsin-Madison, Madison, WI; [7]Department of Anatomy, Cell Biology & Physiology, Indiana University School of Medicine, Indianapolis, IN; [8]Richard L. Roudebush Veterans Affairs Medical Center, Indianapolis, IN

***Current affiliation**: University of California, San Diego

Running title: Estrogen receptor-dependent regulation of apelin and BMPR2 in the RV

Correspondence:

Tim Lahm, MD

Walther Hall, C400

980 W. Walnut St

Indianapolis, IN 46202

Phone: (317) 278-0413

Email: tlahm@iu.edu

Conflict of Interest: No conflicts exist regarding the content of this manuscript. Conflicts unrelated to the content of this manuscript: A. Frump's institution received research funding from Actelion. S. Bonnet served on advisory boards for Actelion, Janssen, Resverlogix. T. Lahm has received consultancy fees from Bayer and Altavant Sciences and was site PI for a clinical trial funded by Complexa.

Abstract

Women with pulmonary arterial hypertension (PAH) exhibit better right ventricular (RV) function and survival than men; however, the underlying mechanisms are unknown. We hypothesized that 17β-estradiol (E2), through estrogen receptor α (ERα), attenuates PAH-induced RV failure (RVF) by up-regulating the pro-contractile and pro-survival peptide apelin *via* a bone morphogenetic protein receptor 2 (BMPR2)-dependent mechanism. We report that ERα and apelin expression are decreased in RV homogenates from patients with RVF and from rats with maladaptive (but not adaptive) RV remodeling. RV cardiomyocyte apelin abundance increased in vivo or in vitro after treatment with E2 or ERα agonist. Studies employing ERα or ERβ null mice, ERα loss-of-function mutant rats or siRNA demonstrated that ERα is necessary for E2 to upregulate RV apelin. E2 and ERα increased BMPR2 in PH-RVs and in isolated RV cardiomyocytes, associated with ERα binding to the *Bmpr2* promoter. BMPR2 is required for E2-mediated increases in apelin abundance, and both BMPR2 and apelin are necessary for E2 to exert RV-protective effects. E2 or ERα agonist rescued monocrotaline-PH and restored RV apelin and BMPR2. We identified a novel cardioprotective E2-ERα-BMPR2-apelin axis in the RV. Harnessing this axis may lead to novel, RV-targeted therapies for PAH patients of either sex.

Introduction

Pulmonary arterial hypertension (PAH) is characterized by dysregulated vasoconstriction, muscularization of pre-capillary arteries, and formation of complex obstructive plexiform lesions in the pulmonary vasculature (1). This leads to increased pulmonary vascular resistance and right ventricular (RV) strain, eventually resulting in the development of RV failure (RVF) (1). Current therapies target vasodilatory pathways in the lung but are not curative (2). Given that RV function is the main determinant of survival in PAH, recent guidelines have called for the development of RV-specific therapies (3, 4). To develop targets for such RV-specific therapies, it is critical to identify modifiers of RV function in PAH.

Even though PAH is sexually dimorphic and more common in women, female PAH patients survive longer than male patients (5, 6). This survival advantage has been attributed to better RV function in females, through as of yet unknown mechanisms (5, 7, 8). Female PAH patients exhibit better contractility, higher RV ejection fraction and better RV-PA coupling than their male counterparts, and recent studies demonstrate that superior RV function contributes to the female survival advantage in PAH (8-10). Sex differences in RV function are mediated at least in part by biologically relevant effects of sex hormones, evidenced by correlations of estrogen levels with RV function in healthy postmenopausal hormone therapy users (7) and by higher cardiac indices in female PAH patients compared with male patients that are not observed in patients older than 45 years (11). These data suggest that to understand sex differences in PAH mortality, it is imperative to decipher the effects of sex hormones on the RV. Ultimately, a better understanding of the molecular mechanisms underlying superior female RV function would be expected to facilitate the development of non-hormonal and RV-specific therapies for patients with PAH and RVF of either sex.

We previously identified the sex steroid 17β-estradiol (E2) as a mediator of pro-contractile, anti-inflammatory and anti-apoptotic effects in the RV (12, 13). These actions translated into

improved RV function and exercise capacity without negatively affecting pulmonary vascular remodeling. Here, we aimed to decipher the yet unidentified mechanisms and downstream mediators of E2's RV-protective effects. We demonstrate that E2 exerts protective effects on RV function and maladaptive remodeling *via* estrogen receptor α (ERα), and identify a mechanism by which ERα activates bone morphogenetic protein receptor 2 (BMPR2) signaling to up-regulate apelin, a potent effector of cardiac contractility (14, 15). While BMPR2 and apelin are required for cardiac development and pulmonary vascular homeostasis (16-19), we now provide evidence that this pathway, *via* ERα, is also functioning in the RV, demonstrating a molecular basis for E2's RV-protective effects.

Results

Evidence of an ERα-apelin signaling axis in human RV

E2 signals through two main receptors, ERα and ERβ (20). We previously showed that E2 as well as ERα-agonist treatment are RV-protective in rat models of PH-induced RVF and that ERα abundance correlates with improved RV adaptation (12, 13). We therefore sought to identify molecular evidence of an E2-ERα signaling axis in RVs from patients with and without RVF (21).

ERα protein was decreased in RV homogenates from male and female patients with RVF compared to controls (**Fig. 1A**). ERβ expression, on the other hand, did not differ between groups (**Suppl. Fig. 1A**). We localized ERα to RV cardiomyocytes (RVCMs) as well as RV endothelial cells (RVECs; **Fig. 1B&C**). In RVCMs, we noted a decrease in abundance of both nuclear as well as cytoplasmic ERα, whereas in RVECs, only cytoplasmic ERα was decreased. No gender differences in ERα or ERβ expression were noted.

In previous studies, E2 repletion in SuHx-PH rats was associated with increased expression of the pro-contractile and pro-survival peptide apelin (12). We therefore evaluated

apelin expression in human RV. We found that RV apelin protein abundance was decreased in RVF *vs.* controls (**Fig. 2A**). Interestingly, in patients with RVF, RV apelin abundance correlated positively with ERα expression and cardiac output (**Fig. 2B&C**). Furthermore, apelin expression correlated negatively with RV fibrosis and RVCM hypertrophy (**Fig. 2D&E**). Similar to ERα, both apelin and its receptor APLNR localized to RVCMs and RVECs (**Fig. 2F&G**). Apelin and APLNR fluorescence intensity were significantly decreased in RVCMs and tended to be decreased in RVECs (**Fig. 2B&C**). No gender differences in apelin or APLNR expression were noted. No correlations were found between ERβ expression and apelin abundance or cardiac output (**Suppl. Fig. 1B&C**). These data suggest an RV-protective ERα-apelin signaling axis in human RVs, with decreased expression of ERα, apelin and APLNR in the setting of RVF.

Apelin is decreased in RVs characterized by maladaptive, but not adaptive, remodeling

To mechanistically study apelin's role in the RV, we evaluated expression of apelin and its receptor in male rat RVs. Apelin and APLNR were strongly expressed in RVCMs and vascular cells, with apelin most strongly expressed in the vasculature and APLNR expressed both in the vasculature and cardiomyocytes (**Fig. 3A**). To evaluate apelin's role in preventing the progression from adaptive to maladaptive RV remodeling, we measured its expression in RV homogenates from male rats with sugen/hypoxia-induced PH (SuHx-PH), monocrotaline-induced PH (MCT-PH) and pulmonary artery banding (PAB) with either maladaptive (characterized by decreased cardiac output, fibrosis, and altered expression of genes involved in fatty acid metabolism and neurohormonal activation; **Suppl. Fig. 2**) or adaptive RV hypertrophy (characterized by preserved cardiac output, lack of fibrosis, and maintained/less profoundly altered gene expression; **Suppl. Fig. 2**). Apelin was decreased in maladaptive but not adaptive (**Fig. 3B**) RV hypertrophy suggesting protective effects of apelin against RVF development. Decreases in apelin were specific to the RV; no alterations in levels were noted in the left ventricle (LV; **Suppl. Fig. 3**).

We next correlated RV apelin expression with mediators of RV structure and function (**Fig. 3C**). RV apelin mRNA correlated negatively with increases in RVSP, RV hypertrophy and pro-apoptotic signaling and positively with cardiac output in male and female rats. Finally, RVCMs isolated from male SuHx-PH rats exhibited decreased apelin protein expression compared to controls (**Fig. 3D**). These data suggest that decreased myocardial apelin is a hallmark of RVF and that apelin may mediate favorable RV adaptations.

RVCM-derived apelin promotes RVEC and RVCM function

Our immunolocalization studies (Fig. 2) suggest that apelin could exert RV-protective effects by targeting RVCMs and/or RVECs. Beneficial effects of apelin in cardiac endothelial cells have been established (22, 23). However, the role of cardiomyocyte apelin is not well defined. Given the decreased expression of apelin and APLNR in RVCMs, we performed studies using conditioned media to delineate the role of RVCM apelin. RVCM apelin was knocked-down by siRNA, the cell culture media collected, and naive RVECs and RVCMs exposed to the conditioned media (**Fig. 4A&B**). Exposure to siRNA apelin conditioned media resulted in decreased RVEC migration and tube formation (**Fig. 4C&D**) as well as decreased RVCM activation of the pro-survival mediator ERK1/2 (24) and decreased expression of the pro-survival and pro-contractile signaling mediator PKCε (25, 26)(**Fig. 4E&F**). Similarly, treatment of RVECs or RVCMs with APLNR antagonist ML221 rendered these cells unresponsive to stimulatory effects of RVCM conditioned media on migration, angiogenesis as well as ERK1/2 activation and PKCε expression (**Suppl. Fig. 4**). These data demonstrate that cardiomyocyte apelin has physiologically relevant paracrine effects on RVECs and RVCMs.

E2 increases apelin expression in RVCMs

We next hypothesized that E2 up-regulates apelin in RVCMs. Since inflammation and cardiomyocyte apoptosis are key features of RVF (27, 28), we evaluated E2's effects on H9c2 cardiomyoblasts stressed with TNF-α or staurosporine (**Fig. 5A&B**). Interestingly, E2 pretreatment attenuated TNF-α or staurosporine-induced decreases in apelin levels (**Fig. 5A&B**). In vivo*,* we found that ovariectomized SuHx-PH females replete with E2 exhibited 40% higher apelin expression in RV homogenates than ovariectomized SuHx-PH females without E2 (**Fig. 5C**). In RVCMs, SuHx-PH induced decreases in apelin were abrogated in cells isolated from male SuHx-PH rats treated with E2 in vivo (**Fig. 5D**). Finally, treatment of RVCMs isolated from male and female SuHx-PH or control rats with E2 in vitro increased apelin protein 1.9- and 3-fold, respectively (**Fig. 5E&F**). These data identify E2 as a potent inducer of apelin in RVCMs.

Apelin signaling is necessary for E2-mediated stimulation of pro-survival signaling in vitro and for E2 to exert RV-protective effects in vivo

We next studied whether E2 stimulates survival signaling in the RV, and whether apelin is necessary for E2 to exert this effect. In RVCMs isolated from male SuHx-PH rats, activation of ERK1/2 was decreased, whereas no such decrease was noted in RVCMs from E2-treated SuHx-PH male rats (**Suppl. Fig. 5A**). Similarly, in H9c2 cells, pretreatment with E2 prevented TNFα-induced decreases in ERK1/2 activation (**Suppl. Fig. 5B**). Knockdown studies demonstrated that E2 increases pro-survival signaling in cardiomyocytes in an apelin-dependent manner (**Suppl. Fig. 5B**).

To study whether apelin signaling is necessary for E2 to exert RV protection in vivo, we treated male PAB rats with E2 ± APLNR antagonist ML221. Indeed, ML221 co-treatment resulted in loss of protective effects of E2 on RV hypertrophy, cardiac output, stroke volume, and

neurohormonal activation (**Suppl. Fig. 6A-E**). Similarly, ML221 co-treatment resulted in decreased RV ERK1/2 activation and PKCε expression as compared to E2 alone (**Suppl. Fig. 6F**). These data indicate that apelin and APLNR signaling are necessary for E2 to exert RV-protection.

ERα is necessary and sufficient to increase apelin

Previous studies in SuHx-PH rats identified correlations between RV ERα expression and apelin mRNA abundance as well as RV structure and function (12). We now expand these findings by demonstrating a robust correlation between ERα and apelin *protein* expression in SuHx-PH RVs (**Fig. 6A**). To evaluate whether this ERα-apelin relationship extends to a large animal model, we studied correlations in RVs from yearling steers with and without high altitude-induced PH. We found robust correlations between ERα and apelin mRNA (**Suppl. Fig. 7A&D**). In conjunction with the data demonstrating a correlation between ERα and apelin protein in human RVs (**Fig. 2B**), these data indicate an ERα-apelin relationship that extends across several species. ERβ, on the other hand, did not correlate with apelin or RV function in human (**Suppl. Fig. 1B&C)** or rat RVs (**Suppl. Fig. 8**).

Next, we investigated whether ERα is necessary for E2-mediated up-regulation of apelin. Using siRNA, we identified that ERα indeed is necessary for E2 to up-regulate apelin in H9c2 cells (**Fig. 6B**). We then treated H9c2 cells with the ERα-selective agonist BTPα (29) and determined that ERα activation is sufficient to induce apelin expression (**Fig. 6C**). This effect extended to RVCMs from healthy male rats, where ex vivo treatment with E2 or BTPα more than doubled apelin abundance (**Fig. 6D**). Similarly, BTPα increased apelin abundance in RVCMs from male and female SuHx-PH rats, albeit to a slightly lesser degree than in RVCMs from healthy rats (**Fig. 6E**). ERα activation was also sufficient to increase apelin in vivo, evidenced by a 30%

increase in RV apelin mRNA expression in male SuHx-PH rats treated with ERα agonist PPT that recapitulated increases seen with E2 treatment (**Fig. 6F**). This increase occurred at the cardiomyocyte level, as RVCMs isolated from SuHx-PH male rats treated with E2 or PPT exhibited increased apelin abundance (**Fig. 6G**). Two distinct in vivo loss-of-function studies solidified these data: First, in RVs from chronically hypoxic E2-treated WT, ERα (*Esr1*), or ERβ (*Esr2*) KO male mice, ERα (but not ERβ) was necessary for E2 to increase apelin (**Fig. 7A**). Second, RV apelin expression was decreased in ERα loss-of-function mutant male and female rats exposed to hypoxia (**Fig. 7B**. ERα mutant rats also exhibited a decrease in cardiac index (*vs.* WT; **Fig. 7C**), suggesting that ERα exerts stimulatory effects on RV function. Together, these data suggest that E2 increases RVCM apelin *via* ERα in vitro and in vivo.

ERα is necessary for E2 to attenuate cardiopulmonary dysfunction in severe PH

Next, we determined if ERα, in addition to being necessary for E2 to increase apelin, is also necessary for E2 to improve cardiopulmonary hemodynamics. We treated male or ovariectomized female WT or ERα loss-of-function mutant SuHx-PH rats with E2. As shown previously, we found that E2 prevented PH-induced cardiopulmonary dysfunction (**Fig. 8A-E**). However, this was not observed in ERα mutant rats, suggesting that ERα indeed is necessary for E2 to exert protective effects in the cardiopulmonary system (**Fig. 8A-E**). As in our in vitro and mouse studies, ERα was indispensable for E2 to increase RV apelin (**Fig. 8F**).

E2 increases BMPR2 in RVCMs

Since BMPR2 increases apelin in the lung vasculature (30), and since the *BMPR2* promoter has an estrogen response element (31), we studied whether BMPR2 is a target of E2 in the RV. BMPR2 was indeed expressed in the RV, with its abundance inversely correlating with

SuHx-induced increases in RVSP (r=-0.66, p=0.01) and RV mass (r=-0.65, p=0.01). Important to our hypothesis, in H9c2 cells, E2 attenuated staurosporine- or TNFα-induced decreases in BMPR2 (**Fig. 9A&B**). E2 also increased BMPR2 in RVCMs isolated from control male or SuHx-PH male and female rats (**Fig. 9C&D**). In vivo, E2 repletion restored SuHx-induced decreases in RV BMPR2 expression from male and female rats (**Fig. 9E**). PH-induced decreases in BMPR2 in RVCMs isolated from SuHx-PH male rats were prevented with in vivo E2 treatment (**Fig. 9F**). These data suggest that E2 increases BMPR2 in RVCMs in vitro and in vivo.

ERα is necessary and sufficient to increase BMPR2

We next determined the role of ERα in E2-mediated increases in BMPR2. In SuHx-PH RVs from male and female rats, ERα protein correlated positively with BMPR2 abundance (**Fig. 10A**). Similarly, a correlation between ERα and BMPR2 mRNA was found in RVs from yearling steers (**Suppl. Fig. 7B+E**).

We then evaluated whether ERα binds to the *Bmpr2* promoter in presence of E2 by performing a ChIP assay in E2-treated H9c2 cells. We detected time-dependent ERα binding to the *Bmpr2* promoter (**Fig. 10B**). Similar to the effect on apelin, we found that in E2-treated H9c2 cells, BMPR2 up-regulation was significantly blunted after ERα knockdown (**Fig. 10C**). Next, we established that treatment with ERα agonist BTPα is sufficient to increase BMPR2 independent of E2 in H9c2 cells (**Fig. 10D**) and RVCMs from control male or SuHx-PH male and female rats (**Fig. 10E&F**). Furthermore, ERα activation also increased expression of the BMPR2 targets p-Smad 1/5/9 and Id1 (**Suppl. Fig. 11A**), suggesting that ERα activation is sufficient to increase canonical BMPR2 signaling. This increase was similar to the increase noted with E2 (**Suppl. Fig. 11B**). In vivo, treatment of male SuHx-PH rats with ERα agonist PPT replicated E2's effects and induced a significant increase in RV BMPR2 (**Fig. 10G**). Finally, RVCMs isolated from male SuHx-

PH rats treated with E2 or PPT in vivo demonstrated abrogated SuHx-induced decreases in BMPR2 (**Fig. 10H**). Taken together, these data demonstrate that ERα binds to the *Bmpr2* promoter, upregulates RVCM BMPR2 expression in vitro and in vivo, and is necessary and sufficient to increase BMPR2. These data also indicate that ERα increases canonical as well as non-canonical BMPR2 downstream signaling.

BMPR2 is necessary for E2 to upregulate apelin and exert cardioprotective effects

In pulmonary artery endothelial cells, BMPR2 promotes formation of a β-catenin/peroxisome proliferator-activated receptor γ (PPARγ) complex that binds to the apelin promoter (30). To evaluate whether E2 stimulates this pathway in cardiac cells, we treated H9c2 cells with E2 and, using co-IP, indeed detected β-catenin/PPARγ complex formation (**Fig. 11A**). We then determined if BMPR2 is necessary for the E2-mediated up-regulation of apelin. Indeed, BMPR2 knockdown in E2-treated H9c2 cells abrogated the E2-mediated up-regulation of apelin (**Fig. 11B**). ERα expression was not affected by BMPR2 knockdown, confirming that ERα is upstream of BMPR2 (**Fig. 11B**). We next measured apelin abundance in H9c2 cells stressed with TNF-α or staurosporine and treated with E2 ± siRNA directed against BMPR2. E2 was unable to maintain apelin expression after BMPR2 knockdown, suggesting that BMPR2 is indeed necessary for E2 to increase apelin (**Fig. 11C&D**). Finally, in stressed cardiomyoblasts, BMPR2 knockdown blocked the E2-mediated up-regulation of phospho-ERK1/2, a known downstream target of apelin (24) (**Fig. 11E**). BMPR2-mediated regulation of apelin was further corroborated by a positive correlation between BMPR2 and apelin mRNA in RVs from yearling steers (**Suppl. Fig. 7C&F**). These data suggest that E2 promotes formation of a β-catenin/PPARγ complex and indicate that BMPR2 is necessary for E2 to increase apelin expression and ERK1/2 phosphorylation. These

findings, in conjunction with data presented in Fig. 9, support the presence of an E2-ERα-BMPR2-apelin axis in the RV.

To study whether BMPR2 is essential for E2 to increase apelin and attenuate RV dysfunction in vivo, we employed male or ovariectomized female rats with a monoallelic deletion of 71 bp in exon 1 of the Bmpr2 gene (*Δ71* rats) (32) and induced RV failure by PAB. We treated subgroups of these rats with E2 and compared E2's effects to those in E2-treated PAB WT controls. E2 increased cardiac output in PAB WT but was unable to do this in *Δ71* rats (**Suppl. Fig. 13A**)**.** Similarly, E2 lowered RV end-diastolic pressure in PAB WT, but was not capable of lowering this parameter in *Δ71* rats (**Suppl. Fig. 13B**). Lastly, E2-treated PAB *Δ71* rats exhibited a significantly prolonged pulmonary artery acceleration time than E2-treated PAB WT rats (**Suppl. Fig. 13C**). While E2 increased RV apelin expression in WT 1.4-fold, E2 was unable to increase RV apelin in *Δ71* rats (**Suppl. Fig. 13D**). These data indicate that BMPR2 is necessary for E2 to attenuate RV dysfunction and increase RV apelin expression in vivo.

E2 or ERα agonist increases RV BMPR2 and apelin and maintains RV adaptation in established PH

To determine if E2 or PPT *reverse* established PH and assess effects of E2 or PPT on the entire cardiopulmonary axis, we used a rescue approach in the MCT-PH model (**Fig. 12A**). Male MCT-PH rats were treated with E2 or PPT starting two weeks after MCT injection. Both E2 or PPT rescued MCT-induced decreases in RV BMPR2 and apelin (**Fig. 12B**). Importantly, E2 or PPT decreased RVSP by 45% (**Fig. 12C**), and RV hypertrophy by 45% and 22%, respectively (**Fig. 12D**). Both compounds, administered when RV adaptation was still preserved, attenuated MCT-induced decreases in cardiac index (CI), resulting in a 60% higher cardiac index than in untreated MCT rats (**Fig. 12E&G**). In fact, E2 or PPT almost normalized total pulmonary resistance index

(**Fig. 12F**). These changes occurred without E2 or PPT attenuating pulmonary vascular remodeling (**Suppl. Fig. 14**). These data indicate that E2 and PPT increase RV BMPR2 and apelin and maintain RV adaptation even in established PH, and that these changes cannot be explained by indirect RV effects from decreased lung vascular remodeling.

E2 exerts direct RV-protective effects that are independent of effects on RV afterload

Protective effects of E2 on RV function could be due to indirect effects from a lower RV afterload. While our studies in isolated RVCMs and PAB rats (**Suppl. Fig. 6 & 13**) demonstrate direct effects of E2 on the RV, we aimed to study E2's RV effects in vivo in more detail. We administered E2 to PAB male rats employing a prevention approach (E2 starting at PAB) as well as a delayed (treatment) approach (E2 starting 4 weeks after PAB; **Fig. 13A**). The prevention approach indeed attenuated PAB-induced increases in RV hypertrophy, and RV end-diastolic diameter (**Fig. 13B-C**). Furthermore, preventative E2 increased RVSP/RV mass compared to untreated PAB (**Fig. 13D**), suggesting a higher force per contractile unit (33). E2-treated rats also exhibited a 3-fold higher stroke volume index (SVI) and a 3-fold higher CI than untreated rats (**Fig. 13E-H**). These changes were associated with decreased neurohormonal activation (**Fig. 13 I-J**) and preservation of RV apelin expression in E2-treated animals (**Fig. 13K**). While effects of the treatment E2 approach were not as robust as those of preventative E2, this strategy resulted in significant ≥50% decreases in RV hypertrophy, RV end-diastolic diameter, and neurohormonal activation (**Fig. 13B-C, I-J**) and a doubling (though not statistically significant) of SVI and CI as compared to untreated controls (**Fig. 13E-H**). These data demonstrate that E2 has direct and afterload-independent effects on RV function and RV apelin expression in vivo.

E2 or ERα agonist prolong survival in experimental PH and RVF

Lastly, we evaluated whether E2 or ERα improve survival in experimental RVF. Indeed, E2 or PPT (*via* a prevention protocol) decreased mortality in SuHx-PH compared to untreated rats (**Suppl. Fig. 15A**). Similarly, in PAB rats, both preventative E2 as well as E2 given *via* a delayed/treatment approach decreased mortality (**Suppl. Fig. 15B**). These data suggest that RV-protective effects of E2 and ERα in the cardiopulmonary axis translate into a robust survival benefit.

Discussion

Our studies identified a cardioprotective E2-ERα-BMPR2-apelin axis in the RV (**Suppl. Fig. 15C**). We describe a mechanism by which E2, *via* ERα, activates BMPR2 signaling to up-regulate apelin, a potent effector of cardiac contractility (16). While apelin is known to exert positive effects on RV function (14, 34), its regulation in the RV is not yet known. Similarly, the role and regulation of BMPR2 in the RV are incompletely understood. While BMPR2 and apelin are required for cardiac development and pulmonary vascular homeostasis (17-19), we now provide evidence that these mediators, employed *via* ERα, are active in the RV, providing a molecular basis for E2's RV-protective effects.

We previously demonstrated that E2 improves cardiac output, decreases RV mass, and favorably affects pro-apoptotic signaling, pro-inflammatory cytokine activation and mitochondrial dysfunction in experimental RVF (12). We also showed that RV ERα expression in healthy females is higher compared to males, tends to decrease with RVF in females and after OVX, increases with E2 repletion, and correlates with markers of RV adaptation. RV ERβ expression, on the other hand, was not affected by sex, PH, or hormone manipulation. We now demonstrate that E2 and ERα increase or maintain BMPR2 and apelin in stressed cardiomyoblasts, in isolated

RVCMs and in RVs from multiple animal models. We also provide evidence that the ERα-apelin signaling axis is active in human RV tissues (Fig. 1&2). We demonstrate that ERα is necessary and sufficient to up-regulate BMPR2 and apelin (Fig. 6, 7&10) and necessary for E2 to mediate RV-protection (Fig. 8). We show that ERα binds to the *Bmpr2* promoter in presence of E2 and that BMPR2 is necessary for RV-protective effects of E2 and for E2-mediated up-regulation of apelin (Fig. 10&11). We demonstrate functionally relevant effects of RVCM apelin (Fig. 4) and establish that apelin is necessary for E2 to exert RV-protective effects (Suppl. Fig. 6). In addition, we identified several other downstream targets of E2 and ERα (ERK1/2, P38MAPK, caspase-3/7; Suppl. Fig. 5, 9&10). We show that treatment with E2 or ERα agonist restores RV apelin and BMPR2 and improves RV structure and function even in established PH (Fig. 12&13). Importantly, E2's RV-protective effects were associated with improved survival (Suppl. Fig. 15).

E2-mediated protection was observed in several models of RV pressure overload. Our studies in MCT-PH and SuHx-PH, while not allowing dissection of RV-specific effects from indirect effects mediated by changes in RV afterload, evaluate "net" effects of E2 and ERα in the entire cardiopulmonary axis. They therefore provide clinically relevant information and identify exogenous E2 and ERα activation as potential therapeutic strategies to attenuate pulmonary vascular and RV dysfunction. Our PAB experiments and studies in isolated RVCMs, on the other hand, demonstrate that E2 and ERα indeed exert *direct* effects on the RV, opening a potential avenue for RV-directed therapies. The signaling pathway described here is of particular interest since it is therapeutically targetable: activators of ERα (29), BMPR2 (35) or apelin (14) already are available and could rapidly be tested in clinical trials.

Our studies employing delayed treatment strategies in MCT-PH and PAB (Figs. 12&13) suggest that E2 can maintain RV adaptation and prevent or prolong the transition to maladaptive RV hypertrophy. While it is puzzling that E2 improved survival in PAB rats without statistically increasing cardiac function, we speculate that the increases in SVI and CI, though not statistically

significant, were sufficient to positively impact survival. Treatment at an earlier time point may have been more efficacious.

ERα is cardioprotective in the LV (36), and loss-of-function mutations in *ESR1* have been linked to myocardial infarction and stroke (37, 38). However, the role of ERα in the RV had not been studied. Importantly, studies from the LV cannot simply be extrapolated to the RV, as both chambers are embryologically, structurally, and physiologically distinct (39). We localized ERα to cardiomyocytes and demonstrate that ERα increases BMPR2 and apelin and attenuates pro-apoptotic signaling in these cells. Co-localization of ERα staining with nuclei (Fig. 1A) and binding of ERα to the *Bmpr2* promoter suggest that ERα signals in the RV *via* genomic mechanisms; however, effects on apelin and BMPR2 were noted within 4h, suggesting that non-genomic mechanisms may occur as well. Effects of ERα may extend beyond cardiomyocytes. In the LV, ERα promotes angiogenesis (40). We detected ERα in RVECs, and studies deciphering the role of ERα in RV angiogenesis are currently underway.

ERα has previously been linked to PH development (41, 42); however, these studies only investigated pulmonary artery (PA) smooth muscle cells and mice with chronic hypoxia (a less robust PH model), thus limiting their generalizability. Increased ERα RNA and *ESR1* SNPs associated with PAH development in humans (43, 44), but these studies do not allow for conclusions regarding ERα's *function*. Our studies demonstrate beneficial effects of ERα in the RV. We previously demonstrated that E2 and ERα agonist treatment improve RV function in SuHx-PH without worsening PA remodeling (12, 13), and we now show that both compounds also rescue established PH and demonstrate beneficial effects on survival. We posit that continuously administering exogenous E2 (especially in absence of endogenous female sex hormones, as seen in OVX or in male animals) or selectively activating ERα are strategies to harness RV-protective effects of estrogenic signaling in PAH without negatively affecting PA remodeling. Continuous E2 administration may be superior to endogenous release as it avoids fluctuations in

levels, which may be associated with negative effects in the PA (41). This could also explain why aromatase inhibition may be beneficial in PAH (42, 45). However, concern exists that aromatase inhibition negatively affects RV function (46). We posit that administering exogenous E2 or ERα agonist in context of a "low female sex steroid environment" (e.g. in post-menopausal female or male patients or in premenopausal females after inhibiting endogenous hormones) is safer and more efficacious than inhibiting aromatase, but this hypothesis remains to be tested. Importantly, ERα-selective agonist treatment confers cardiovascular protection without unwanted uterotrophic effects (47).

While estrogens affect clinical outcomes in PAH, and while female gender is associated with a survival benefit in this disease, additional factors such as other sex hormones and age also are modifiers of outcomes (48). This may explain why the survival difference between male and female patients in the REVEAL cohort is driven by males >60 years (49). Interactions between gender, age and the distinct patient population enrolled in REVEAL may explain the specific observations in this cohort. REVEAL also demonstrated a higher female:male ratio compared to other registries, suggesting that patients in this cohort may be distinct from other PAH populations (49). This may result from enrollment of individuals with higher wedge pressures or different comorbidities.

Upstream regulators and downstream targets of BMPR2 in the RV are incompletely understood. In the lung, BMPR2 induces apelin (30), and decreased activation of the BMPR2-apelin axis causes PAH (30). While the role of BMPR2 signaling in RVF had been unstudied until recently, evolving evidence suggests relevant RV effects. First, absence of BMPR2 during cardiac development causes RV outflow tract malformations (17, 18). Second, PAH patients with *BMPR2* mutations exhibit more profound RVF than patients without a mutation (50). Third, *BMPR2*-mutant cardiomyoblasts and RVs from *BMPR2*-mutant mice exhibit abnormalities in fatty acid oxidation (51) as well as calcium signaling and cell contractility (32). We now expand the current knowledge

by identifying BMPR2 as a target of E2/ERα in RVCMs. Binding of ERα to the *Bmpr2* promoter and formation of β-catenin/PPARγ complexes after E2 treatment suggest that E2, *via* ERα, increases BMPR2, and that BMPR2, *via* β-catenin/PPARγ, increases apelin. This does not rule out that ERα directly interacts with apelin as well; however, apelin expression was profoundly decreased after BMPR2 knockdown (Fig. 11B). Since E2 treatment resulted in β-catenin/PPARγ complex formation and given the recently observed RV-protective effects of PPARγ activation (52), it is also conceivable that stimulatory effects on PPARγ signaling and fatty acid oxidation contribute to E2's RV protection. Our data suggest that E2/ERα may also employ canonical BMPR2 signaling (Suppl. Fig. 11&12). Ongoing investigations are evaluating how BMPR2 expression and signaling are decreased in RVF. Mechanisms could include decreased BMPR2 synthesis, increased BMPR2 turnover and/or upregulation of BMPR2 inhibitors. Our studies in *Δ71* rats (Suppl. Fig. 13) suggest that BMPR2 indeed is necessary for RV-protective effects of E2 in vivo. Future studies will evaluate time courses, different degrees of BMPR2 loss-of-function and larger animal numbers.

Our findings of stimulatory effects of E2/ERα on BMPR2 contradict a paradigm where E2 decreases BMPR2 expression in PA smooth muscle cells or lymphocytes (53, 54). We believe that such a paradigm is overly simplistic. E2 is pleiotropic, and discrepancies between studies could result from dose-, context- and compartment-specific effects. Of note, we also detected stimulatory effects of E2 and ERα on BMPR2 in PA endothelial cells (55). Studies in specific cell types are necessary to further dissect effects of estrogenic signaling on BMPR2. Our studies suggest that E2 and ERα can increase BMPR2 and that the "net" effect of E2 or ERα activation in experimental PH is salutary (Figs. 8&12; Suppl. Fig. 15).

Apelin, *via* APLNR, exerts pro-contractile, pro-angiogenic and anti-apoptotic effects in the LV (56). Emerging data suggest a role for apelin in the RV: APLNR knockout mice exhibit dilated and/or deformed RVs, apelin knockout mice exhibit exaggerated PH, and circulating apelin is

decreased in PAH patients (57, 58). Apelin is an inotrope in the RV (15, 34) and is decreased in SuHx-PH RVs (12, 59). Short-term infusion of Pyr-apelin-13 reduces pulmonary vascular resistance and increases cardiac output in PAH patients (14). Our human RV data link apelin to less RV fibrosis and hypertrophy (Fig. 2D&E). However, mechanisms and regulators of apelin-mediated RV-protective signaling are unknown. We identified two previously unidentified regulators of RV apelin and provide mechanistic evidence linking apelin to better RV function.

While prior studies indicated that apelin is predominantly expressed in endothelial cells (22, 23) , we now provide evidence that apelin is also expressed in rat and human RVCMs (Figs. 2F&G, 3D), that apelin is decreased in RVCMs from RVF patients (Fig. 2F), and that RVCM-derived apelin exerts paracrine and potentially autocrine effects on pro-angiogenic effects in RVECs as well as stimulatory effects on pro-contractile and pro-survival signaling in RVCMs (Fig. 4; Suppl. Fig. 4). Interestingly, recent studies employing single-cell RNA Seq in human or mouse hearts also demonstrated that apelin is expressed in several cardiomyocyte populations (60, 61). Our data suggest that the presence of apelin may not be limited to endothelial cells and that RVCM apelin may also exert physiologically relevant effects. Studies of ERα-BMPR2-apelin signaling in other cell types, such as RVECs or pulmonary artery endothelial cells are currently underway.

Our study has limitations. First, H9c2 cardiomyoblasts are not RV-specific. However, we confirmed results obtained in these cells in vivo and in isolated RVCMs. This suggests that, given the limitations of primary cardiomyocyte culture, H9c2 cells are appropriate for mechanistic studies, as long as results are corroborated in cardiomyocytes and/or in vivo. Second, studies in human RV tissue were limited by lack of tissue from disease-free controls and lack of cardiac output data from all individuals. Differences between RVF patients and healthy controls may be more pronounced; however, RV tissue from healthy subjects is not available. Third, apelin loss-of-function studies employed pharmacologic blockade of APLNR rather than genetic

manipulation. However, studies in transgenic animals would have required mice, which would be limited by lack of a robust RVF phenotype (3). Experiments using a rat model therefore are more clinically relevant. Future studies will specifically evaluate the role of cardiomyocyte apelin in vivo (along with cardiomyocyte ERα and BMPR2). Fourth, while we employed several methods to determine that apelin is expressed and functionally relevant in RVCMs, and while apelin expression was identified through single-cell RNA-Seq (60, 61), the most definite method to establish a functional role of RVCM apelin would be through development of an RVCM-specific loss-of-function rodent model. We will focus on such studies in the future. Finally, correlations between ERα and apelin expression in human RV could only be established in RVF patients. Interestingly, ERα expression in control hearts was more variable. This could be due to the patients' gender, age, or other unknown modifiers. However, the ERα-apelin correlation during RVF was robust and corroborated in several animal models. While hemodynamic or echocardiographic data were not available for all subjects, occurrence of RVF was clinically adjudicated and confirmed at autopsy.

In summary, we identified a molecular mechanism of E2 and ERα-mediated attenuation of RVF in PAH. We identified BMPR2 and apelin as regulators of pro-survival and adaptive signaling in the RV and as targets of E2 and ERα. Harnessing this cardioprotective E2-ERα-BMPR2-apelin axis may allow for developing non-hormonal and RV-directed therapies for PAH patients of either sex.

Materials and Methods

General

All experiments were performed in accordance with recent recommendations (3, 62), including randomization and blinding at the time of measurement and analysis.

Animal models

Sugen/hypoxia-induced PH (SuHx-PH): Su5416 (20 mg/kg subcutaneously; dissolved in DMSO; Sigma Aldrich, St. Louis, MO) was administered immediately prior to hypoxia exposure. Hypoxia exposure occurred in a hypobaric chamber for 3 weeks, followed by room air exposure for 4 weeks (12). Experimental groups included intact male and female age-matched Sprague-Dawley normoxic controls, intact male and female SuHx-PH rats, ovariectomized (OVX; described previously (12)) SuHx-PH females, and OVX SuHx-PH females replete with E2 (75 µg/kg/d *via* subcutaneous pellets [resulting in physiological levels (12)]; Innovative Research of America; Sarasota, FL). Males weighed 175-200 g; females weighed 150-175 g (Charles River; Wilmington, MA). Additional studies were performed in male SuHx-PH rats with or without E2 (75 µg/kg/day; subcutaneous pellets) or ERα-selective agonist 4,4',4''-(4-Propyl-[1H]-pyrazole-1,3,5-triyl)trisphenol (PPT; 850 µg/kg/day*;* subcutaneous pellets (12)). Vehicle for E2 or PPT did not have any effects on cardiopulmonary parameters in prior studies and was not included in the current analysis (63).

Hypoxia-induced PH (HPH): Male and female age-matched Sprague-Dawley rats containing loss-of-function mutations in *Esr1* (encoding ERα) and their wildtype (WT) littermate controls were exposed to 3 weeks of normobaric hypoxia (equivalent to 10% O_2). Experimental detail and validation of *Esr1* mutations are found in **Suppl. Table 1** & **Suppl. Fig. 16**. In addition, male WT, *Esr1*$^{-/-}$ and *Esr2*$^{-/-}$ (encoding ERβ) C57BL/6 mice (20-22 g; Jackson Laboratories) were

exposed to 3 weeks of hypobaric hypoxia while treated with E2 (75 μg/kg/d; subcutaneous pellets).

Monocrotaline-induced PH (MCT-PH): Male Sprague-Dawley rats (200-250 g) were subcutaneously injected with MCT (60 mg/kg; Sigma Aldrich). Two weeks later, subgroups of animals received E2 (75 μg/kg/day) or PPT (850 μg/kg/day) for two more weeks *via* subcutaneous pellets, followed by endpoint analysis.

Pulmonary artery banding (PAB): Male Sprague-Dawley rats (150-180 g) were anesthetized by inhaled isoflurane and orotracheally intubated. A small incision was made through the intercostal muscle and extended toward the sternum and the spine, and the thoracic cavity opened. The PA was then dissected, and a 4-0 silk suture was passed around the PA and, using 19G needle hub, constricted. The thoracic cavity was then closed, re-evacuated and monitored for re-filling of air, and muscle layers sutured. Sham controls underwent identical surgical procedure without PA constriction. Additional studies were performed in male PAB rats with E2 (75 μg/kg/day; subcutaneous pellets) given at the time of surgery (preventative group) or 4 weeks after surgery, when cardiac output began to decrease (treatment group).

RNA-Seq of bovine RV

RNA-Seq was performed in RV tissue from yearling steers and data deposited in the NIH GEO repository, Ascension number GSE164320. See supplemental methods for experimental detail.

Human RV tissue

Human RV free wall tissue was collected as described previously (21, 64) from warm autopsies (<3 hours following death) or cardiac surgery. The RVF group was comprised of patients with congenital heart disease without LV involvement and patients with idiopathic or scleroderma-associated end-stage PAH (age 49.9±5.5 years; 70% female). RVF was defined as

decreased tricuspid annular plane systolic excursion and/or death from RVF (21). The presence of RVF was confirmed during autopsy. Control group tissues were obtained from donors with coronary artery disease or aortic stenosis without evidence of PAH or RV hypertrophy by echocardiography or histological analysis (21, 64) (45.1±3.8 years; 77% female). Clinical characteristics are described in **Suppl. Table 2**.

RV cardiomyocyte (RVCM) isolation

RVCMs were isolated using the Adult Rat/Mouse Cardiomyocyte Isolation Kit (Cellutron Life Technologies, Baltimore, MD). Hearts were perfused *via* a simplified Langendorff system and Cole-Parmer MasterFlex peristaltic pump (Vernon Hills, IL) at 8 ml/min per the manufacturer's guidelines. After perfusion, the RV was dissected and digested. ~$3x10^5$ viable RVCMs (**Suppl. Fig. 17**) were seeded in a laminin-coated 6-well plate and maintained in AS media-containing serum (Cellutron). Cells were maintained for at least 6h after isolation prior to treatment. Experiments were performed within 24h after isolation.

Statistics

Results are expressed as means±SEM. At least three biologically independent experiments (run in technical duplicates) were performed for all in vitro studies and reported as N. Statistical analyses were performed with GraphPad Prism 6 (La Jolla, CA). Sample sizes were estimated by power calculation. 2-tailed Student's t-test or one-way ANOVA with Tukey's or Dunnett's post-hoc correction were used for comparison of experimental groups. Correlations were determined using Pearson's coefficient (R). Statistically significant difference was accepted at $p<0.05$.

Study approval

All human studies were performed in accordance with Laval University and Institute Universitaire de Cardiologie et de Pneumologie de Québec biosafety and human ethics (CER-

20773). All patients or their legal representatives (in case of autopsy) gave informed consent before beginning of the study.

All rodents used were approved by the Indiana University School of Medicine or Laval University Institutional Animal Care and Use Committees (protocols #11220 & 2018-015-2) and were adherent with NIH guidelines for care and use of laboratory animals.

See supplemental data for additional methods.

Author contributions

ALF - designed, performed, and analyzed studies and wrote manuscript; MA, BY, BR - performed experiments; VN, ET, SB-B, FP, JO - performed and analyzed experiments and provided data; ET, SB, AF, ALF, TC - performed hemodynamic and echocardiographic experiments, RDB, KRS - performed and provided bovine RNA-Seq data; CDR, KK, RL, XS, NCC, TL - generated ERα mutant rats; DMT, NCC - hypoxic ERα mutant rat studies; SP, SB - provided human RV tissue and edited manuscript; TL - designed and analyzed studies and wrote and edited manuscript.

Acknowledgements

We thank Dr. Robert G. Presson, Jr for equipment support, the Indiana University School of Medicine Research Immunohistochemistry Facility for technical support, Drs. Henry Bryant and Jeffrey Dodge at Eli Lilly & Co. for academic use of BTPα, Dr. Frederic Perros for providing *Δ71* rats, and Dr. Chiemela Ubagharagi, Emily Seiden, Fatiha Iqbal, and Jiajun Li for technical support. Dr. Frump is supported by AHA Career Development Award 19CDA34660173, ALA Catalyst Award CA-629145, and Actelion Entelligence Young Investigator Award and was previously supported by AHA Postdoctoral Fellowship 17POST33670365 and CTSI Postdoctoral Fellowship 5TL1TR001107-02 (NIH/NCATS). Dr. Lahm is supported by AHA 17GRNT33690017, VA Merit Review Award 2 I01 BX002042-05, NHLBI 1R56HL134736-01A1 and NIH HL144727-01A1. Dr. Stenmark is supported by NHLBI PPG P01 HL014985, NHLBI R01HL114887, and DoD PR140977. Drs. Bonnet and Provencher are supported by CRIUCPQ and by the Canadian Institutes of Health Research. Dr. Bonnet is supported by the Heart and Stroke Foundation of Canada.

References

1. Rabinovitch M. Molecular pathogenesis of pulmonary arterial hypertension. *J Clin Invest.* 2012;122(12):4306-13.

2. Lajoie AC, Lauziere G, Lega JC, Lacasse Y, Martin S, Simard S, et al. Combination therapy versus monotherapy for pulmonary arterial hypertension: a meta-analysis. *Lancet Respir Med.* 2016;4(4):291-305.

3. Lahm T, Douglas IS, Archer SL, Bogaard HJ, Chesler NC, Haddad F, et al. Assessment of Right Ventricular Function in the Research Setting: Knowledge Gaps and Pathways Forward. An Official American Thoracic Society Research Statement. *Am J Respir Crit Care Med.* 2018;198(4):e15-e43.

4. Vonk Noordegraaf A, Chin KM, Haddad F, Hassoun PM, Hemnes AR, Hopkins SR, et al. Pathophysiology of the right ventricle and of the pulmonary circulation in pulmonary hypertension: an update. *Eur Respir J.* 2019;53(1).

5. Humbert M, Sitbon O, Yaici A, Montani D, O'Callaghan DS, Jais X, et al. Survival in incident and prevalent cohorts of patients with pulmonary arterial hypertension. *Eur Respir J.* 2010;36(3):549-55.

6. Lahm T, Tuder RM, and Petrache I. Progress in solving the sex hormone paradox in pulmonary hypertension. *Am J Physiol Lung Cell Mol Physiol.* 2014;307(1):L7-26.

7. Ventetuolo CE, Ouyang P, Bluemke DA, Tandri H, Barr RG, Bagiella E, et al. Sex hormones are associated with right ventricular structure and function: The MESA-right ventricle study. *Am J Respir Crit Care Med.* 2011;183(5):659-67.

8. Jacobs W, van de Veerdonk MC, Trip P, de Man F, Heymans MW, Marcus JT, et al. The right ventricle explains sex differences in survival in idiopathic pulmonary arterial hypertension. *Chest.* 2014;145(6):1230-6.

9. Swift AJ, Capener D, Hammerton C, Thomas SM, Elliot C, Condliffe R, et al. Right ventricular sex differences in patients with idiopathic pulmonary arterial hypertension characterised by magnetic resonance imaging: pair-matched case controlled study. *PLoS One.* 2015;10(5):e0127415.

10. Tello K, Richter MJ, Yogeswaran A, Ghofrani HA, Naeije R, Vanderpool R, et al. Sex Differences in Right Ventricular-Pulmonary Arterial Coupling in Pulmonary Arterial Hypertension. *Am J Respir Crit Care Med.* 2020;202(7):1042-6.

11. Ventetuolo CE, Praestgaard A, Palevsky HI, Klinger JR, Halpern SD, and Kawut SM. Sex and hemodynamics in pulmonary arterial hypertension. *Eur Respir J.* 2013.

12. Frump AL, Goss KN, Vayl A, Albrecht M, Fisher AJ, Tursunova R, et al. Estradiol Improves Right Ventricular Function In Rats With Severe Angioproliferative Pulmonary Hypertension: Effects Of Endogenous And Exogenous Sex Hormones. *Am J Physiol Lung Cell Mol Physiol.* 2015:ajplung.00006.2015.

13. Lahm T, Frump AL, Albrecht ME, Fisher AJ, Cook TG, Jones TJ, et al. 17beta-Estradiol mediates superior adaptation of right ventricular function to acute strenuous exercise in female rats with severe pulmonary hypertension. *Am J Physiol Lung Cell Mol Physiol.* 2016;311(2):L375-88.

14. Brash L, Barnes GD, Brewis MJ, Church AC, Gibbs SJ, Howard L, et al. Short-Term Hemodynamic Effects of Apelin in Patients With Pulmonary Arterial Hypertension. *JACC Basic Transl Sci.* 2018;3(2):176-86.

15. Dai T, Ramirez-Correa G, and Gao WD. Apelin increases contractility in failing cardiac muscle. *Eur J Pharmacol.* 2006;553(1-3):222-8.

16. Szokodi I, Tavi P, Foldes G, Voutilainen-Myllyla S, Ilves M, Tokola H, et al. Apelin, the novel endogenous ligand of the orphan receptor APJ, regulates cardiac contractility. *Circ Res.* 2002;91(5):434-40.

17. Delot EC, Bahamonde ME, Zhao M, and Lyons KM. BMP signaling is required for septation of the outflow tract of the mammalian heart. *Development.* 2003;130(1):209-20.

18. Beppu H, Malhotra R, Beppu Y, Lepore JJ, Parmacek MS, and Bloch KD. BMP type II receptor regulates positioning of outflow tract and remodeling of atrioventricular cushion during cardiogenesis. *Dev Biol.* 2009;331(2):167-75.

19. Kidoya H, and Takakura N. Biology of the apelin-APJ axis in vascular formation. *J Biochem.* 2012;152(2):125-31.

20. Austin ED, Lahm T, West J, Tofovic SP, Johansen AK, Maclean MR, et al. Gender, sex hormones and pulmonary hypertension. *Pulm Circ.* 2013;3(2):294-314.

21. Potus F, Ruffenach G, Dahou A, Thebault C, Breuils-Bonnet S, Tremblay E, et al. Downregulation of MicroRNA-126 Contributes to the Failing Right Ventricle in Pulmonary Arterial Hypertension. *Circulation.* 2015;132(10):932-43.

22. Liu Q, Hu T, He L, Huang X, Tian X, Zhang H, et al. Genetic targeting of sprouting angiogenesis using Apln-CreER. *Nat Commun.* 2015;6:6020.

23. Sheikh AY, Chun HJ, Glassford AJ, Kundu RK, Kutschka I, Ardigo D, et al. In vivo genetic profiling and cellular localization of apelin reveals a hypoxia-sensitive, endothelial-centered pathway activated in ischemic heart failure. *Am J of Physiol Heart and Circ Physiol.* 2008;294(1):H88-H98.

24. Bai B, Tang J, Liu H, Chen J, Li Y, and Song W. Apelin-13 induces ERK1/2 but not p38 MAPK activation through coupling of the human apelin receptor to the Gi2 pathway. *Acta Biochim Biophys Sin (Shanghai).* 2008;40(4):311-8.

25. Perjés Á, Skoumal R, Tenhunen O, Kónyi A, Simon M, Horváth IG, et al. Apelin increases cardiac contractility via protein kinase Cε- and extracellular signal-regulated kinase-dependent mechanisms. *PloS one.* 2014;9(4):e93473-e.

696 26. Szokodi I, Tavi P, Földes G, Voutilainen-Myllylä S, Ilves M, Tokola H, et al. Apelin, the
697 novel endogenous ligand of the orphan receptor APJ, regulates cardiac contractility. *Circ Res.*
698 2002;91(5):434-40.
699 27. Bogaard HJ, Abe K, Vonk Noordegraaf A, and Voelkel NF. The right ventricle under
700 pressure: cellular and molecular mechanisms of right-heart failure in pulmonary hypertension.
701 *Chest.* 2009;135(3):794-804.
702 28. Tuder RM, Archer SL, Dorfmuller P, Erzurum SC, Guignabert C, Michelakis E, et al.
703 Relevant issues in the pathology and pathobiology of pulmonary hypertension. *J Am Coll Cardiol.*
704 2013;62(25 Suppl):D4-12.
705 29. Chalmers MJ, Wang Y, Novick S, Sato M, Bryant HU, Montrose-Rafizdeh C, et al.
706 Hydrophobic Interactions Improve Selectivity to ERalpha for Ben-zothiophene SERMs. *ACS Med*
707 *Chem Lett.* 2012;3(3):207-10.
708 30. Alastalo TP, Li M, Perez Vde J, Pham D, Sawada H, Wang JK, et al. Disruption of
709 PPARgamma/beta-catenin-mediated regulation of apelin impairs BMP-induced mouse and
710 human pulmonary arterial EC survival. *J Clin Invest.* 2011;121(9):3735-46.
711 31. Bourdeau V, Deschenes J, Metivier R, Nagai Y, Nguyen D, Bretschneider N, et al.
712 Genome-wide identification of high-affinity estrogen response elements in human and mouse.
713 *Mol Endocrinol.* 2004;18(6):1411-27.
714 32. Hautefort A, Mendes-Ferreira P, Sabourin J, Manaud G, Bertero T, Rucker-Martin C, et
715 al. Bmpr2 Mutant Rats Develop Pulmonary and Cardiac Characteristics of Pulmonary Arterial
716 Hypertension. *Circulation.* 2019;139(7):932-48.
717 33. Neto-Neves EM, Frump AL, Vayl A, Kline JA, and Lahm T. Isolated heart model
718 demonstrates evidence of contractile and diastolic dysfunction in right ventricles from rats with
719 sugen/hypoxia-induced pulmonary hypertension. *Physiol Rep.* 2017;5(19).
720 34. Yang P, Read C, Kuc RE, Buonincontri G, Southwood M, Torella R, et al. Elabela/Toddler
721 Is an Endogenous Agonist of the Apelin APJ Receptor in the Adult Cardiovascular System, and

722 Exogenous Administration of the Peptide Compensates for the Downregulation of Its Expression
723 in Pulmonary Arterial Hypertension. *Circulation.* 2017;135(12):1160-73.
724 35. Long L, Ormiston ML, Yang X, Southwood M, Graf S, Machado RD, et al. Selective
725 enhancement of endothelial BMPR-II with BMP9 reverses pulmonary arterial hypertension. *Nat*
726 *Med.* 2015;21(7):777-85.
727 36. Murphy E. Estrogen signaling and cardiovascular disease. *Circ Res.* 2011;109(6):687-96.
728 37. Schuit SC, Oei HH, Witteman JC, Geurts van Kessel CH, van Meurs JB, Nijhuis RL, et al.
729 Estrogen receptor alpha gene polymorphisms and risk of myocardial infarction. *J Am Med Assoc.*
730 2004;291(24):2969-77.
731 38. Ardelt AA, McCullough LD, Korach KS, Wang MM, Munzenmaier DH, and Hurn PD.
732 Estradiol Regulates Angiopoietin-1 mRNA Expression Through Estrogen Receptor-α in a Rodent
733 Experimental Stroke Model. *Stroke.* 2005;36(2):337-41.
734 39. Haddad F, Hunt SA, Rosenthal DN, and Murphy DJ. Right ventricular function in
735 cardiovascular disease, part I: Anatomy, physiology, aging, and functional assessment of the right
736 ventricle. *Circulation.* 2008;117(11):1436-48.
737 40. van Rooij E, Fielitz J, Sutherland LB, Thijssen VL, Crijns HJ, Dimaio MJ, et al. Myocyte
738 enhancer factor 2 and class II histone deacetylases control a gender-specific pathway of
739 cardioprotection mediated by the estrogen receptor. *Circ Res.* 2010;106(1):155-65.
740 41. Wright AF, Ewart MA, Mair K, Nilsen M, Dempsie Y, Loughlin L, et al. Oestrogen receptor
741 alpha in pulmonary hypertension. *Cardiovasc Res.* 2015;106(2):206-16.
742 42. Mair KM, Wright AF, Duggan N, Rowlands DJ, Hussey MJ, Roberts S, et al. Sex-
743 dependent influence of endogenous estrogen in pulmonary hypertension. *Am J Respir Crit Care*
744 *Med.* 2014;190(4):456-67.
745 43. Rajkumar R, Konishi K, Richards TJ, Ishizawar DC, Wiechert AC, Kaminski N, et al.
746 Genomewide RNA expression profiling in lung identifies distinct signatures in idiopathic

pulmonary arterial hypertension and secondary pulmonary hypertension. *Am J Physiol Heart Circ Physiol.* 2010;298(4):H1235-48.

44. Roberts KE, Fallon MB, Krowka MJ, Brown RS, Trotter JF, Peter I, et al. Genetic risk factors for portopulmonary hypertension in patients with advanced liver disease. *Am J Respir Crit Care Med.* 2009;179(9):835-42.

45. Kawut SM, Archer-Chicko CL, DeMichele A, Fritz JS, Klinger JR, Ky B, et al. Anastrozole in Pulmonary Arterial Hypertension. A Randomized, Double-Blind, Placebo-controlled Trial. *Am J Respir Crit Care Med.* 2017;195(3):360-8.

46. Lahm T, and Frump AL. Toward Harnessing Sex Steroid Signaling as a Therapeutic Target in Pulmonary Arterial Hypertension. *Am J Respir Crit Care Med.* 2017;195(3):284-6.

47. Bolego C, Rossoni G, Fadini GP, Vegeto E, Pinna C, Albiero M, et al. Selective estrogen receptor-alpha agonist provides widespread heart and vascular protection with enhanced endothelial progenitor cell mobilization in the absence of uterotrophic action. *FASEB J.* 2010;24(7):2262-72.

48. Badlam JB, and Austin ED. Beyond oestrogens: towards a broader evaluation of the hormone profile in pulmonary arterial hypertension. *Eur Resp J.* 2018;51(6):1801058.

49. Benza RL, Miller DP, Gomberg-Maitland M, Frantz RP, Foreman AJ, Coffey CS, et al. Predicting Survival in Pulmonary Arterial Hypertension. *Circulation.* 2010;122(2):164-72.

50. van der Bruggen CE, Happe CM, Dorfmuller P, Trip P, Spruijt OA, Rol N, et al. Bone Morphogenetic Protein Receptor Type 2 Mutation in Pulmonary Arterial Hypertension: A View on the Right Ventricle. *Circulation.* 2016;133(18):1747-60.

51. Talati MH, Brittain EL, Fessel JP, Penner N, Atkinson J, Funke M, et al. Mechanisms of Lipid Accumulation in the Bone Morphogenetic Protein Receptor Type 2 Mutant Right Ventricle. *Am J Respir Crit Care Med.* 2016;194(6):719-28.

52. Legchenko E, Chouvarine P, Borchert P, Fernandez-Gonzalez A, Snay E, Meier M, et al. PPARgamma agonist pioglitazone reverses pulmonary hypertension and prevents right heart failure via fatty acid oxidation. *Sci Transl Med.* 2018;10(438).

53. Austin ED, Hamid R, Hemnes AR, Loyd JE, Blackwell T, Yu C, et al. BMPR2 expression is suppressed by signaling through the estrogen receptor. *Biol Sex Differ.* 2012;3(1):6.

54. Mair KM, Yang XD, Long L, White K, Wallace E, Ewart MA, et al. Sex affects bone morphogenetic protein type II receptor signaling in pulmonary artery smooth muscle cells. *Am J Respir Crit Care Med.* 2015;191(6):693-703.

55. Frump AL, Yakubov B, Albrecht M, Comhair SAA, Erzurum SC, Tabima Martinez D, et al. American Thoracic Society; 2019:A7399-A.

56. Dalzell JR, Rocchiccioli JP, Weir RA, Jackson CE, Padmanabhan N, Gardner RS, et al. The Emerging Potential of the Apelin-APJ System in Heart Failure. *J Card Fail.* 2015;21(6):489-98.

57. Kang Y, Kim J, Anderson JP, Wu J, Gleim SR, Kundu RK, et al. Apelin-APJ signaling is a critical regulator of endothelial MEF2 activation in cardiovascular development. *Circ Res.* 2013;113(1):22-31.

58. Chandra SM, Razavi H, Kim J, Agrawal R, Kundu RK, de Jesus Perez V, et al. Disruption of the apelin-APJ system worsens hypoxia-induced pulmonary hypertension. *Arterioscler Thromb Vasc Biol.* 2011;31(4):814-20.

59. Drake JI, Bogaard HJ, Mizuno S, Clifton B, Xie B, Gao Y, et al. Molecular signature of a right heart failure program in chronic severe pulmonary hypertension. *Am J Respir Cell Mol Biol.* 2011;45(6):1239-47.

60. Hu P, Liu J, Zhao J, Wilkins BJ, Lupino K, Wu H, et al. Single-nucleus transcriptomic survey of cell diversity and functional maturation in postnatal mammalian hearts. *Genes & Development.* 2018.

61. Tucker Nathan R, Chaffin M, Fleming Stephen J, Hall Amelia W, Parsons Victoria A, Bedi Kenneth C, et al. Transcriptional and Cellular Diversity of the Human Heart. *Circulation.* 2020;142(5):466-82.

62. Provencher S, Archer SL, Ramirez FD, Hibbert B, Paulin R, Boucherat O, et al. Standards and Methodological Rigor in Pulmonary Arterial Hypertension Preclinical and Translational Research. *Circ Res.* 2018;122(7):1021-32.

63. Lahm T, Albrecht M, Fisher AJ, Selej M, Patel NG, Brown JA, et al. 17beta-Estradiol attenuates hypoxic pulmonary hypertension via estrogen receptor-mediated effects. *Am J Respir Crit Care Med.* 2012;185(9):965-80.

64. Omura J, Habbout K, Shimauchi T, Wu WH, Breuils-Bonnet S, Tremblay E, et al. Identification of The Long Non-Coding RNA H19 as a New Biomarker and Therapeutic Target in Right Ventricular Failure in Pulmonary Arterial Hypertension. *Circulation.* 2020.

Figures and Figure Legends

Figure 1.

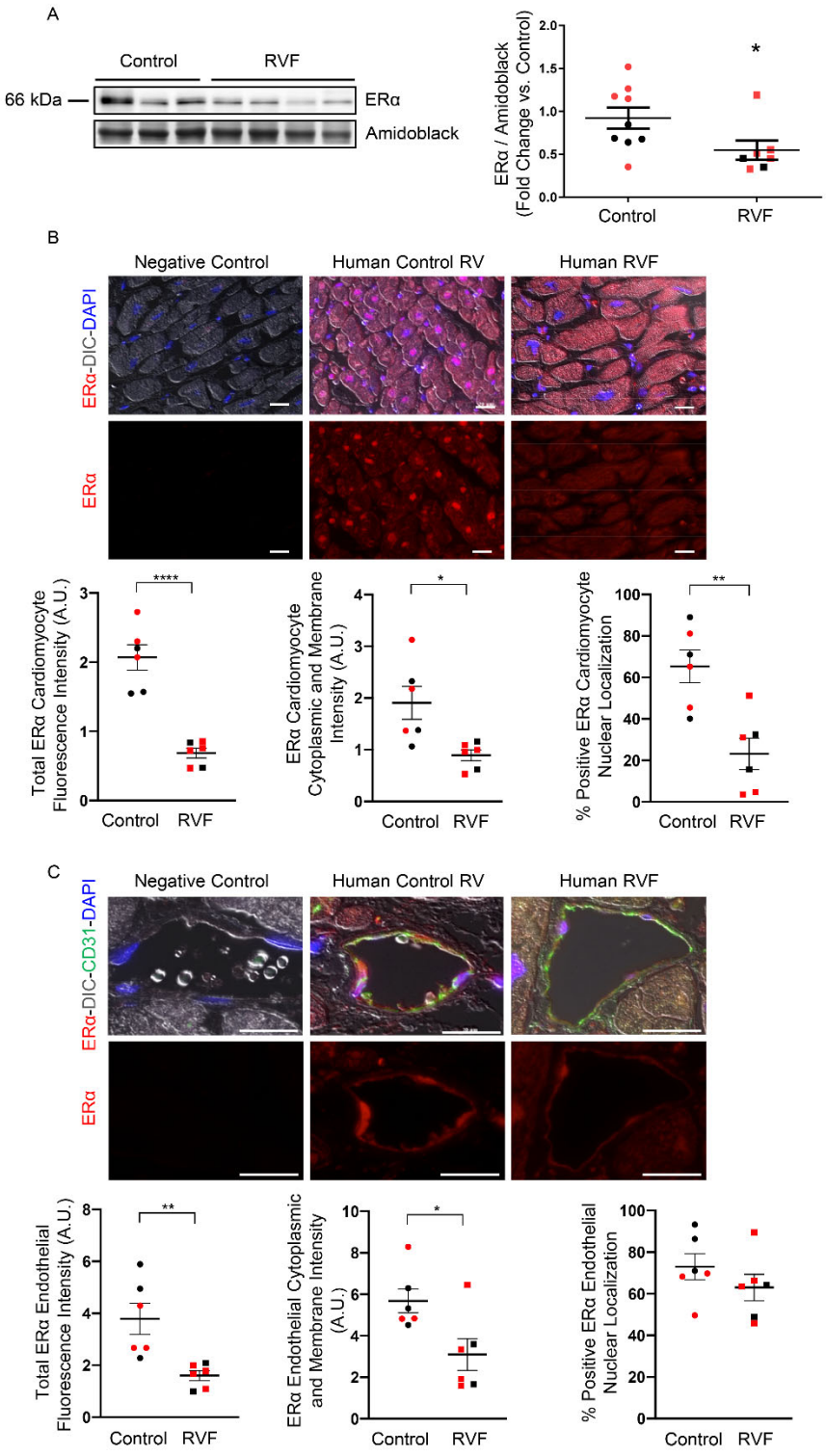

Figure 1. ERα localizes to cardiomyocytes and endothelial cells in human RV and is less abundant in patients with RV failure. (**A**) ERα expression in human RV measured by Western blot. Quantification by densitometry shown on right. (**B**) Representative immunocytochemistry images of RV cardiomyocyte ERα expression and localization in human control RVs and RVs from patients with RV failure (RVF). Cardiomyocyte localization was established by differential interference contrast (DIC). Quantification of total ERα fluorescence intensity, cytoplasmic and membrane fluorescence intensity, and nuclear localization (co-localization with DAPI) is shown in graphs. Images are at 20x magnification; scale bar is 20 μm. (**C**) Representative immunocytochemistry images of ERα expression and localization in RV endothelial cells in human control RVs and RVs from patients with RVF. Endothelial cell localization was established by co-localization with CD31. Total ERα fluorescence intensity, cytoplasmic and membrane fluorescence intensity, and nuclear localization (co-localization with DAPI) are quantified in graphs. Images are at 40x, scale bars are 20 μm. Red and black symbols in graphs represent samples from female and male patients, respectively. Error bars represent means ± SEM. *p<0.05, **p<0.01, ****p<0.0001 vs control by Student's t-test.

Figure 2.

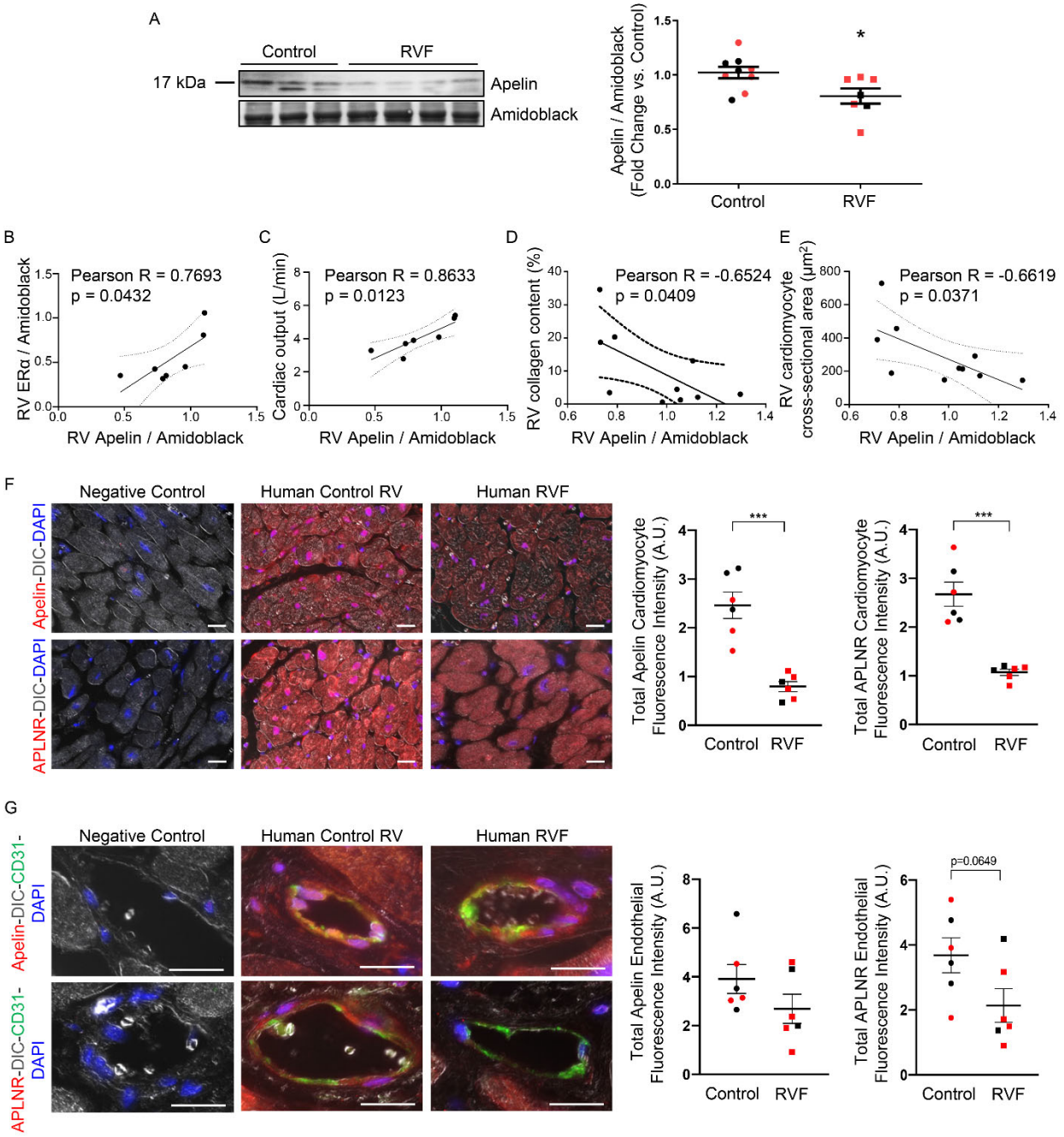

Figure 2. RV cardiomyocyte apelin and apelin receptor (APLNR) expression are decreased in patients with RV failure. (**A**) Apelin expression in human RV tissue measured by Western blot. Quantification by densitometry shown on right. (**B-E**) Apelin expression correlates positively with ERα protein (**B**) and cardiac output (**C**) in RVs from patients with RV

failure (RVF) and negatively with RV collagen content (**D**; expressed as % of RV cross-section) and RV cardiomyocyte size (**E**; measured as cardiomyocyte cross-sectional area [CSA]) in human control RVs and RVs from RVF patients. Cardiac output data was available for RVF patients only. RV collagen content and RV cardiomyocyte size were analyzed in a randomly selected subgroup of control subjects. (**F**) Representative immunocytochemistry images of cardiomyocyte apelin and APLNR expression in human control RVs and RVs from patients with RVF. Cardiomyocyte localization was established by differential interference contrast (DIC). Cardiomyocyte apelin or APLNR fluorescence intensity is quantified in graphs. Images are at 20x magnification; scale bars are 20 μm. (**G**) Representative immunocytochemistry images of endothelial cell apelin and APLNR expression and localization in human control RVs and RVs from patients with RVF. Endothelial cell localization was established by co-localization with CD31. Apelin or APLNR fluorescence intensity is quantified in graphs. Images are at 40x, scale bars are 20 μm. Red and black symbols in graphs represent female and male samples respectively. (A,F-G) *p<0.05, ***p<0.001 vs control by Student's t-test. Error bars represent means ± SEM. (B-E) Pearson's R-value and p-value shown. Dashed lines represent 95%-confidence intervals.

873 **Figure 3.**

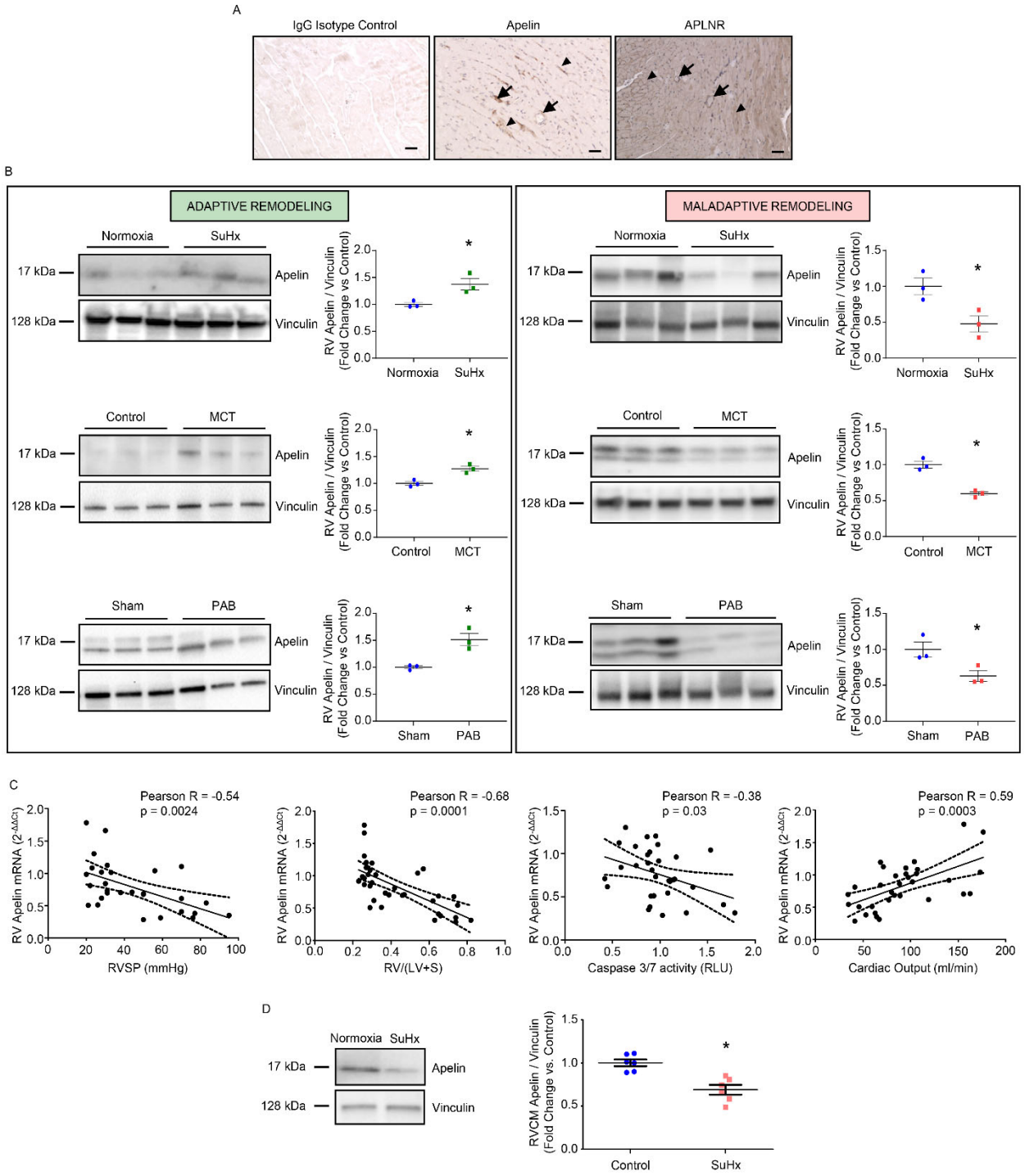

874

875

Figure 3. RV apelin expression is decreased in maladaptive (but not adaptive) RV hypertrophy and correlates negatively with markers of worsening RV function. (**A**) Apelin and APLNR are expressed in the RV. Apelin (middle image) and APLNR (right image) stained by immunohistochemistry in RV of a male Sprague-Dawley rat. Both apelin and APLNR are expressed in coronary endothelial cells (arrows) as well as cardiomyocytes (arrowheads). Images are 10x; scale bars = 50 μm. (**B**) Apelin expression by Western blot and quantified via densitometric analyses in RVs from rats with adaptive remodeling (characterized by preserved cardiac output; left panel) or maladaptive remodeling (characterized by reduced cardiac output; right panel) employing rats with SuHx-PH, monocrotaline-induced PH (MCT), or pulmonary artery banding (PAB). Note decrease in apelin in maladaptive but not adaptive RV hypertrophy. N=3 male rats/group. (**C**) Apelin mRNA correlates negatively with RV systolic pressure (RVSP), RV hypertrophy [RV weight divided by weight of left ventricle + septum; RV/(LV+S)], and pro-apoptotic signaling (caspase-3/7 activity; in relative light units [RLU]), but positively with cardiac output in male and female control rats and rats with SuHx-PH (hemodynamics described in (14)). (**D**) Apelin expression in RV cardiomyocytes (RVCMs) isolated from normoxia control or SuHx-PH male and female rats. A representative Western blot is shown on the left; densitometry is shown on the right. *$p<0.05$ by Student's t-test in (B&D). Error bars in (B&D) represent means ± SEM; each data point represents one animal. Correlation analyses in (C) performed by determining Pearson's correlation coefficient (R) and two-tailed p-value. Dashed lines represent 95% confidence intervals.

Figure 4.

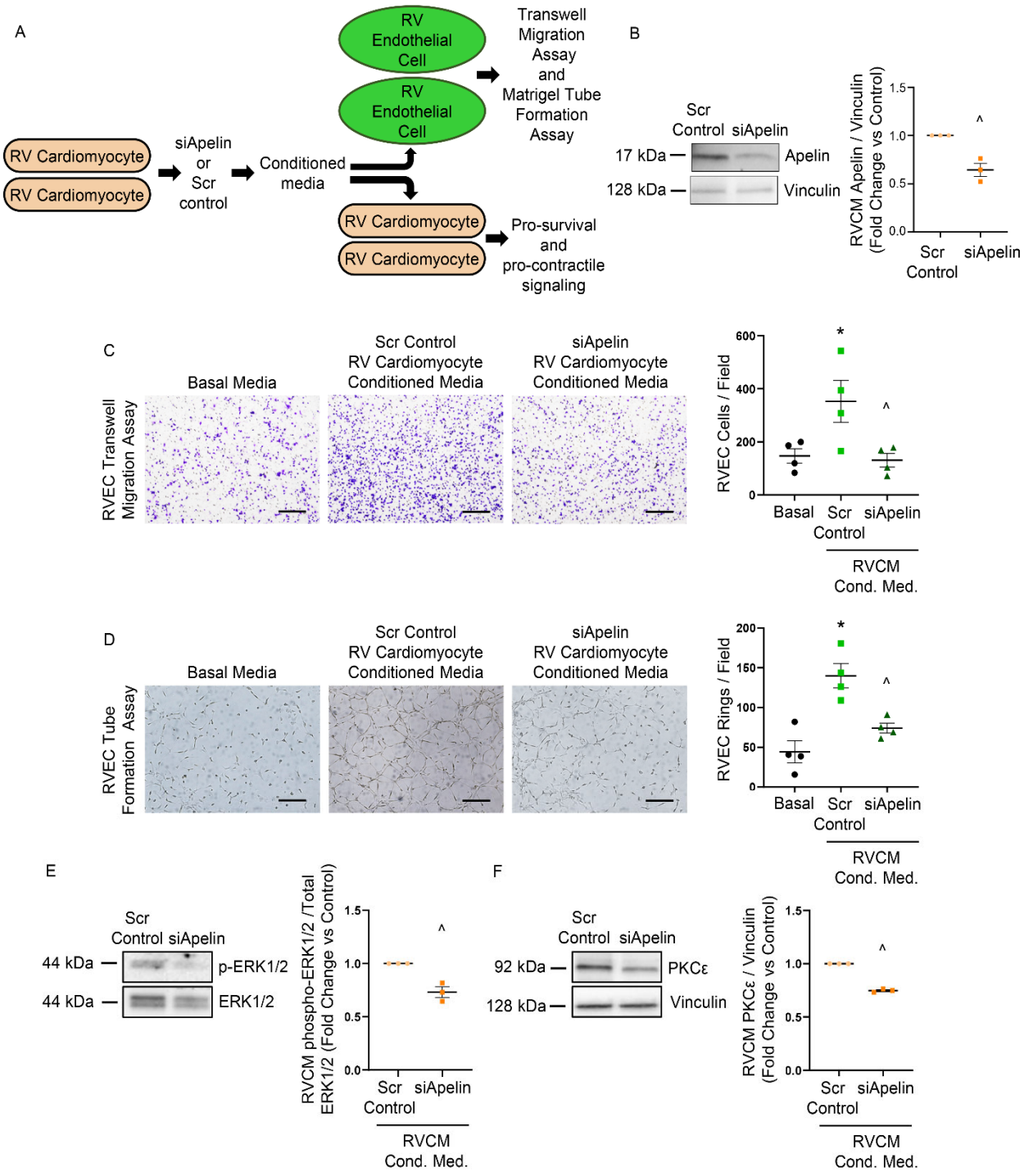
A
RV Cardiomyocyte
RV Cardiomyocyte
siApelin or Scr control
Conditioned media
RV Endothelial Cell
RV Endothelial Cell
Transwell Migration Assay and Matrigel Tube Formation Assay
RV Cardiomyocyte
RV Cardiomyocyte
Pro-survival and pro-contractile signaling
B
Scr Control siApelin
17 kDa
Apelin
128 kDa
Vinculin
RVCM Apelin / Vinculin (Fold Change vs Control)
Scr Control
siApelin
C
Basal Media
Scr Control RV Cardiomyocyte Conditioned Media
siApelin RV Cardiomyocyte Conditioned Media
RVEC Transwell Migration Assay
RVEC Cells / Field
Basal
Scr Control
siApelin
RVCM Cond. Med.
D
Basal Media
Scr Control RV Cardiomyocyte Conditioned Media
siApelin RV Cardiomyocyte Conditioned Media
RVEC Tube Formation Assay
RVEC Rings / Field
E
Scr Control siApelin
44 kDa
p-ERK1/2
44 kDa
ERK1/2
RVCM phospho-ERK1/2 /Total ERK1/2 (Fold Change vs Control)
F
Scr Control siApelin
92 kDa
PKCε
128 kDa
Vinculin
RVCM PKCε / Vinculin (Fold Change vs Control)

Figure 4. RV cardiomyocyte (RVCM) apelin exerts paracrine effects on RV endothelial cell (RVEC) and RVCM function. (**A**) RVCMs were transfected with siRNA directed against apelin (siApelin) or scrambled control (Scr control). 24h later, conditioned media was collected from RVCMs and added to naïve RVECs or RVCMs. RVEC function and RVCM mediators of pro-survival and pro-contractile signaling were then assessed. (**B**) Validation of apelin siRNA knockdown in RVCMs. Scrambled siRNA oligo served as control. N= 3 male rats. (**C**) Transwell migration assay in RVECs treated with RVCM conditioned media after treatment with siApelin or scrambled control. EBM2 media served as baseline control. 15 fields per condition were quantified 16h after conditioned media was added. Representative transwell migration assay images are shown, with quantification on the right. Images are at 10x magnification, scale bars are 250 μm. N = RVECs from 4 male rats, performed in technical triplicate. (**D**) Tube formation assay in RVECs treated with RVCM conditioned media after treatment with siApelin or scrambled control. EBM2 media served as baseline control. Cells plated at a density of $5x10^4$ in technical triplicate. Images taken at 10x magnification; scale bars are 250 μm. Rings quantified using 15 fields per condition. Representative images are shown, with quantification of ring formation depicted on the right. N = RVECs from 4 male rats (in technical triplicate). (**E, F**) Quantification of ERK1/2 activation and PKCε expression in RVCMs treated with RVCM conditioned media after treatment with siApelin or scrambled control. Representative Western blot images are shown, with quantification by densitometry depicted on the right. N = RVCMs from 3 male rats. *$p<0.05$ vs basal media control, ^$p<0.05$ vs Scr control by (C&D) one-way ANOVA with post-hoc Tukey's correction or (E&F) by Student's t-test. Error bars represent means ± SEM; each data point represents cells from one animal.

Figure 5.

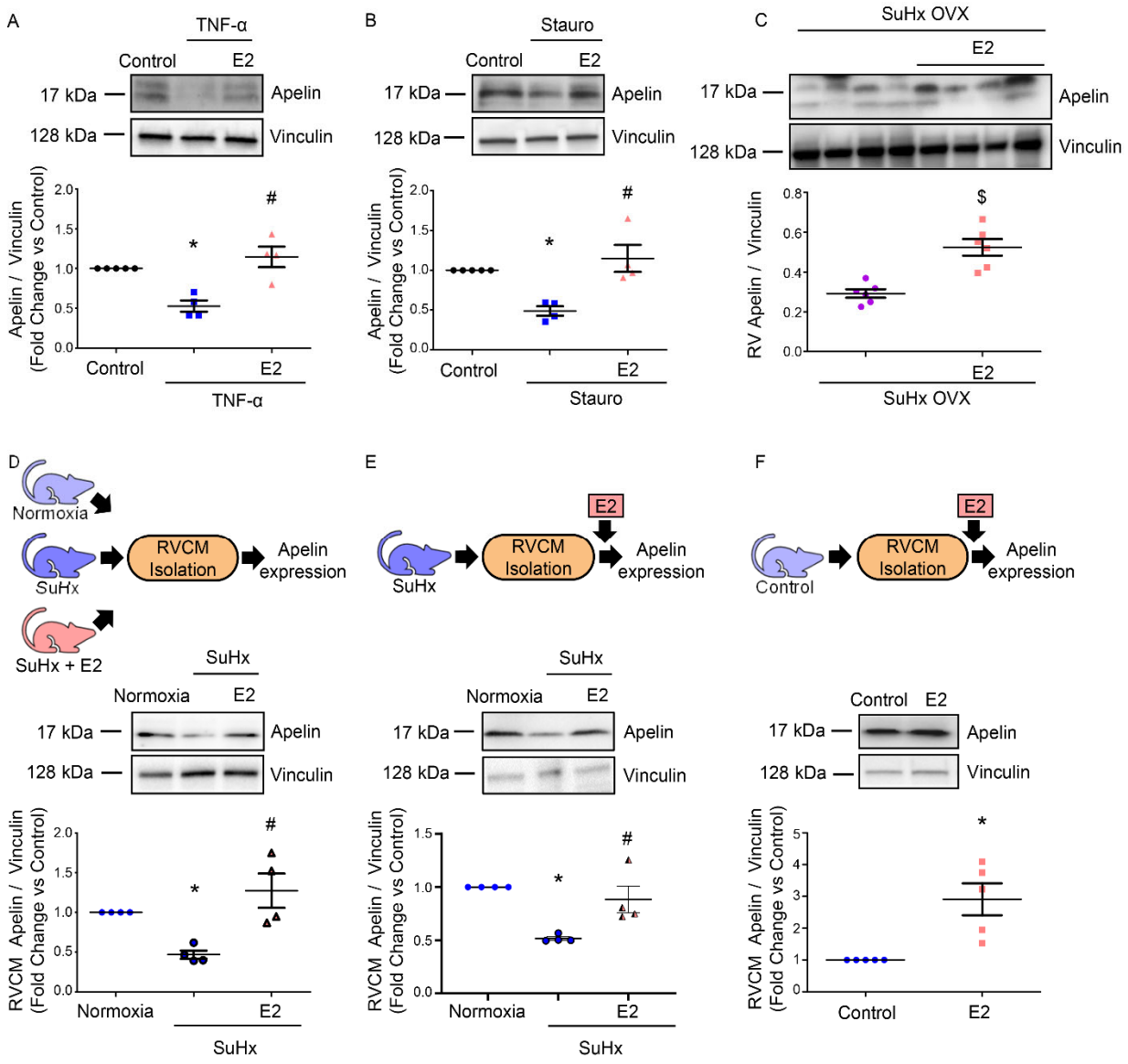

Figure 5. 17β-estradiol (E2) increases apelin expression in stressed cardiomyoblasts, in the failing RV and in isolated RV cardiomyocytes (RVCMs). (A, B) H9c2 rat cardiomyoblasts were pretreated with E2 (100 nM, 24h) and then stressed with TNF-α (10ng/ml, 8h; A) or staurosporine (stauro; 50 nM, 4h; B). **(C)** RVs from female SuHx OVX (ovariectomized SuHx-PH females) or SuHx OVX + E2 (ovariectomized SuHx-PH females replete with E2 75

μg/kg/day via subcutaneous pellets) analyzed for apelin expression by Western blot. (**D**) Apelin expression evaluated by Western blot in RVCMs isolated from male normoxia control, untreated SuHx-PH, and SuHx-PH rats treated with E2 (75 μg/kg/day; subcutaneous pellets) in vivo. (**E**) Western blot analysis of apelin expression in RVCMs isolated from male and female SuHx-PH rats and treated exogenously with E2 (10 nM, 24h). (**F**) Western blot analysis of apelin expression in RVCMs isolated from control male rats treated with E2 (10 nM, 24h) in vitro. N=4 independent experiments in (A, B), N=6 rats/group in (C), cardiomyocytes isolated from N=4-5 rats/group in (D-F), with each data point indicating one animal. All panels demonstrate representative Western blots with densitometric analyses for all experiments or animals. *$p<0.05$ vs control/normoxia; $^{\#}p<0.05$ vs TNF-treated (A), stauro-treated (B) or untreated SuHx (D, E); $^{\$}p<0.05$ vs OVX. p-values in (A, B, D, E) by ANOVA with Dunnett's post-hoc correction; p-values in (C, F) by Student's t-test. Error bars represent means ± SEM; each data point represents one experiment or animal.

Figure 6.

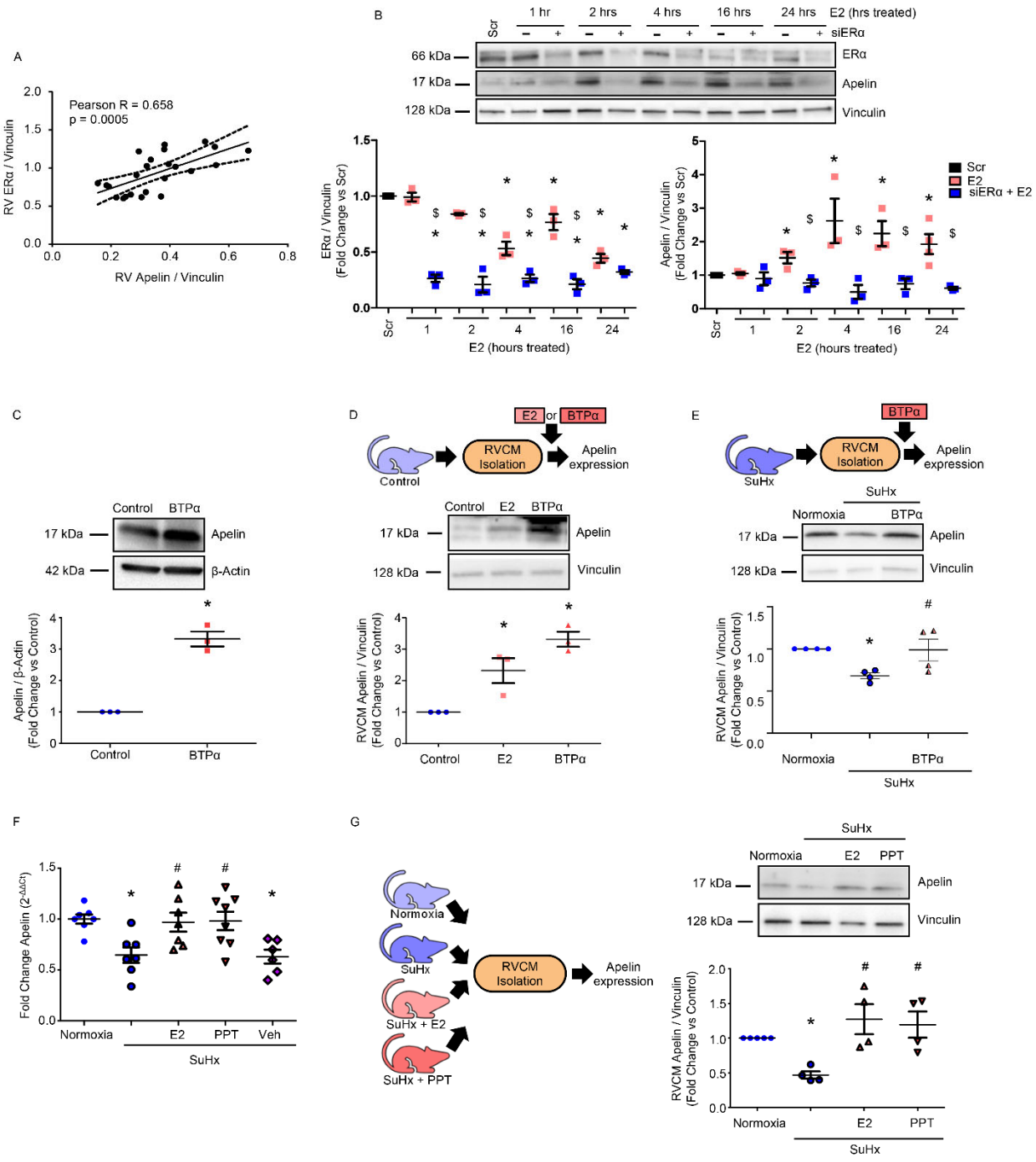

Figure 6. ERα is necessary and sufficient for upregulating apelin in vitro. (A) RV apelin and ERα protein positive correlate in male and female control and SuHx-PH rats. **(B)** ERα siRNA knockdown time-course in H9c2 cardiomyoblasts (5nM; 24h prior to E2 [100 nM]). **(C)** Apelin

expression in H9c2 cells treated with ERα agonist BTPα (100 nM, 24h). **(D)** Apelin expression in RV cardiomyocytes (RVCMs) isolated from male control rats treated with E2 (10 nM, 24h) or BTPα (100 nM, 24h) in vitro. **(E)** Apelin expression in RVCMs isolated from male and female SuHx-PH rats and treated with BTP (100 nM, 24h) in vitro. **(F)** RV apelin mRNA expression in normoxia, SuHx-PH, or SuHx-PH rats treated with E2 (75 μg/kg/day via subcutaneous pellets), ERα agonist PPT (850 μg/kg/day; subcutaneous pellets) or EtOH vehicle (Veh). **(G)** Apelin expression in RVCMs isolated from male controls, SuHx-PH, or SuHx-PH rats treated with E2 or PPT in vivo. N=3 independent experiments for (B&C). Cells from N=3-4 rats/group in (D-E; G). N=6-8/group in (F). (B-E, G) depict representative Western blots with densitometric analyses. Pearson's R-value and p-value shown in (A). Dashed lines represent 95%-confidence intervals. *p<0.05 vs. Scr (scrambled control), $p<0.05 vs. E2 in (B); *p<0.05 vs. control in (C&D); *p<0.05 vs. Normoxia, #p<0.05 vs. SuHx in (E-G). p-values by ANOVA with Tukey's post-hoc correction in (B, D-G) and by Student's t-test in (C). Error bars represent means ± SEM; each data point represents one experiment or animal.

Figure 7

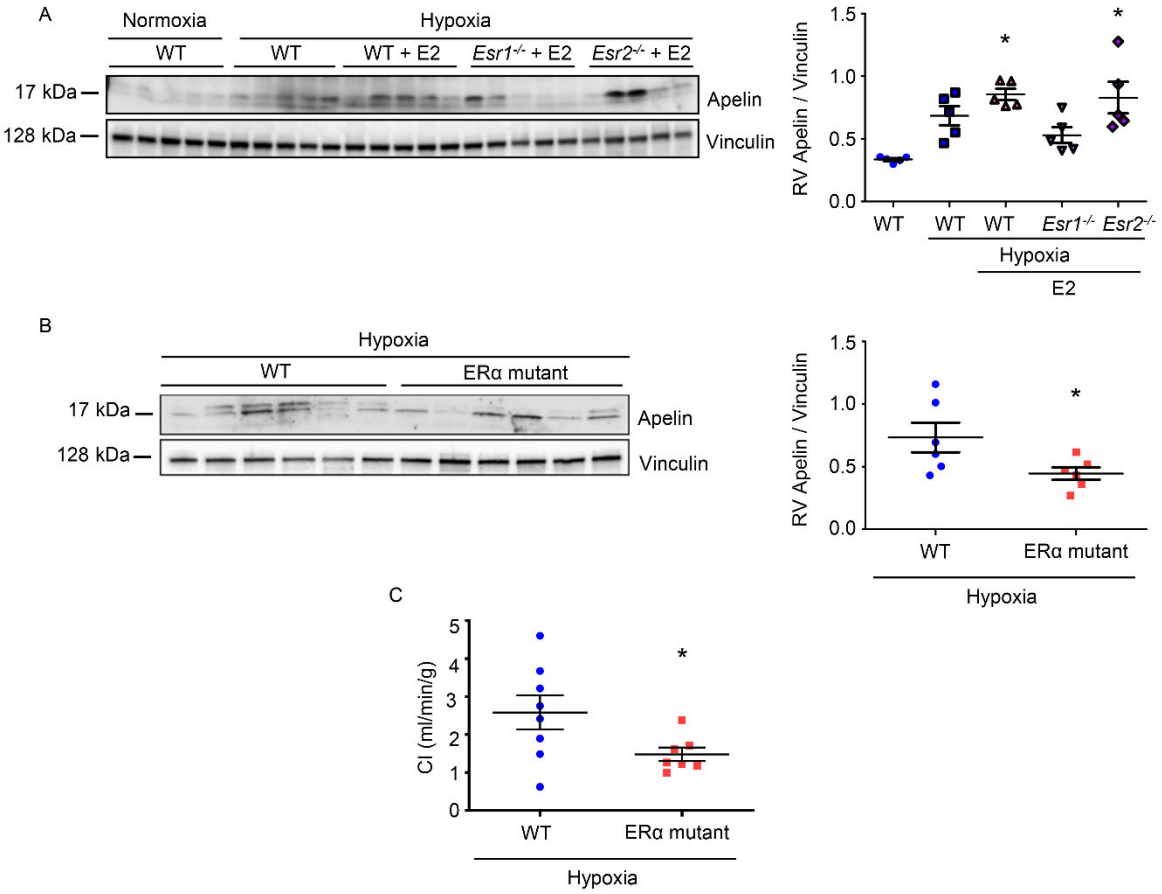

Figure 7. ERα is necessary for upregulating apelin in vivo. (A) RV apelin expression in male wild-type (WT), ERα (Esr1) or ERβ (Esr2) knockout mice with hypoxia-induced PH (HPH) treated with E2 (75 μg/kg/day; subcutaneous pellets). **(B)** RV apelin expression and **(C)** cardiac indices (CI; echocardiographic cardiac output / body weight) in male and female control and ERα (Esr1) mutant HPH rats. N=5/group in (A), N=6/group in (B&C). *p<0.05 vs. WT. p-values by ANOVA with Tukey's post-hoc correction in (A) and by Student's t-test in (B&C). Error bars represent means ± SEM; each data point represents one experiment or animal.

Figure 8.

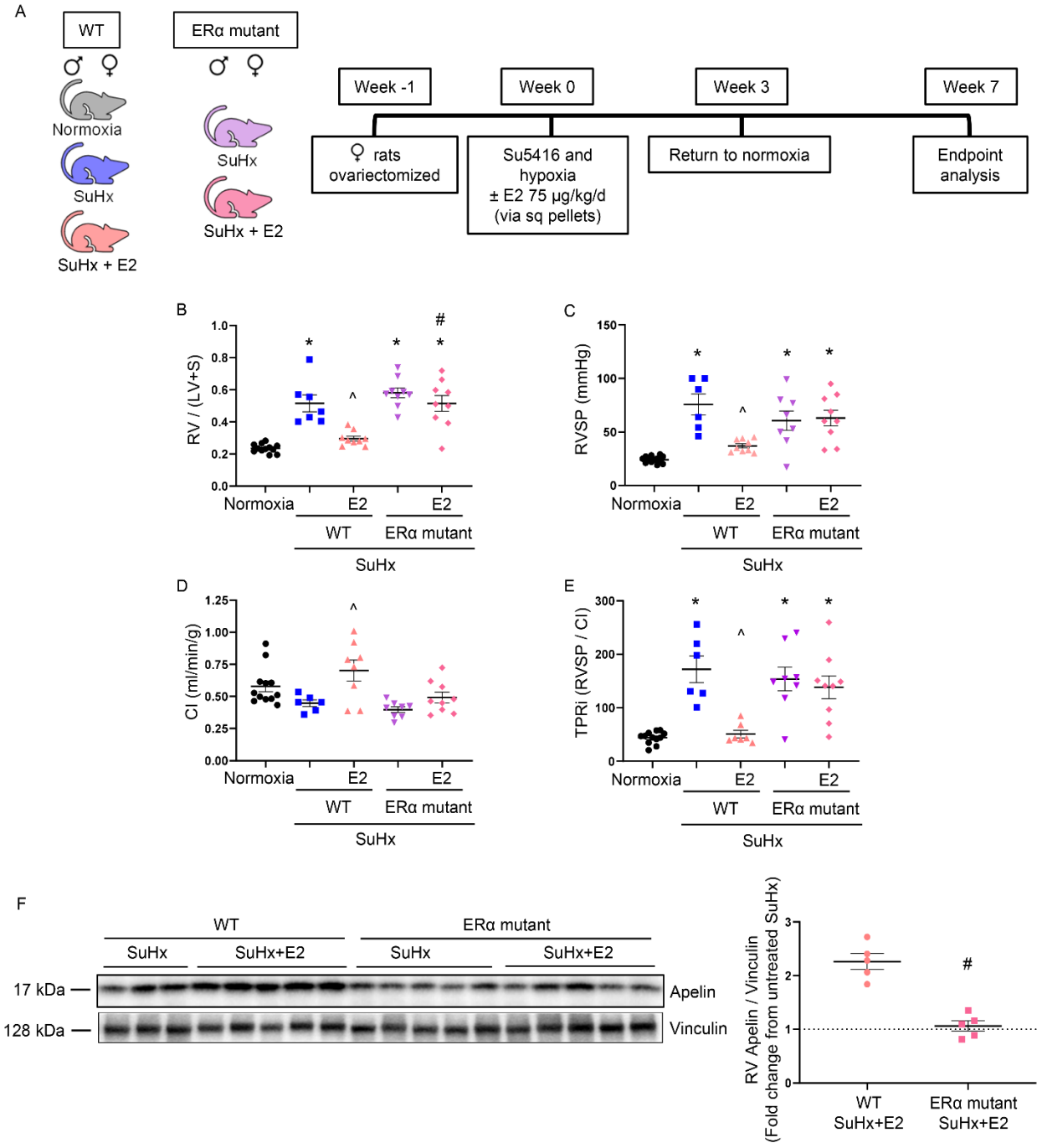

Figure 8. ERα is necessary for E2 to attenuate cardiopulmonary dysfunction in SuHx-PH. (**A**) Experimental design. (**B-E**) Effects of E2 treatment in WT or ERα loss-of-function mutants on RV hypertrophy (RV weight divided by weight of left ventricle plus septum; RV / [LV+S]; **B**),

RV systolic pressure (RVSP; **C**), cardiac index (CI; echocardiographic cardiac output / body weight; **D**), and total pulmonary resistance index (cardiac index / RVSP; **E**). (**F**) Western blot analysis of RV apelin. Densitometric analysis demonstrates decreased ability of E2 to mediate increase in RV apelin in ERα loss-of-function mutant (data expressed as fold-change increase in RV apelin with E2 vs untreated). *p<0.05 vs. normoxia control, ^p<0.05 vs. WT SuHx untreated, #p<0.05 vs. WT SuHx+E2 by one-way ANOVA with Tukey post-hoc correction in (B-E). #p<0.05 vs. WT SuHx+E2 by t-test in (F). Error bars represent means ± SEM. Each data point represents one animal. Sq = subcutaneous.

Figure 9.

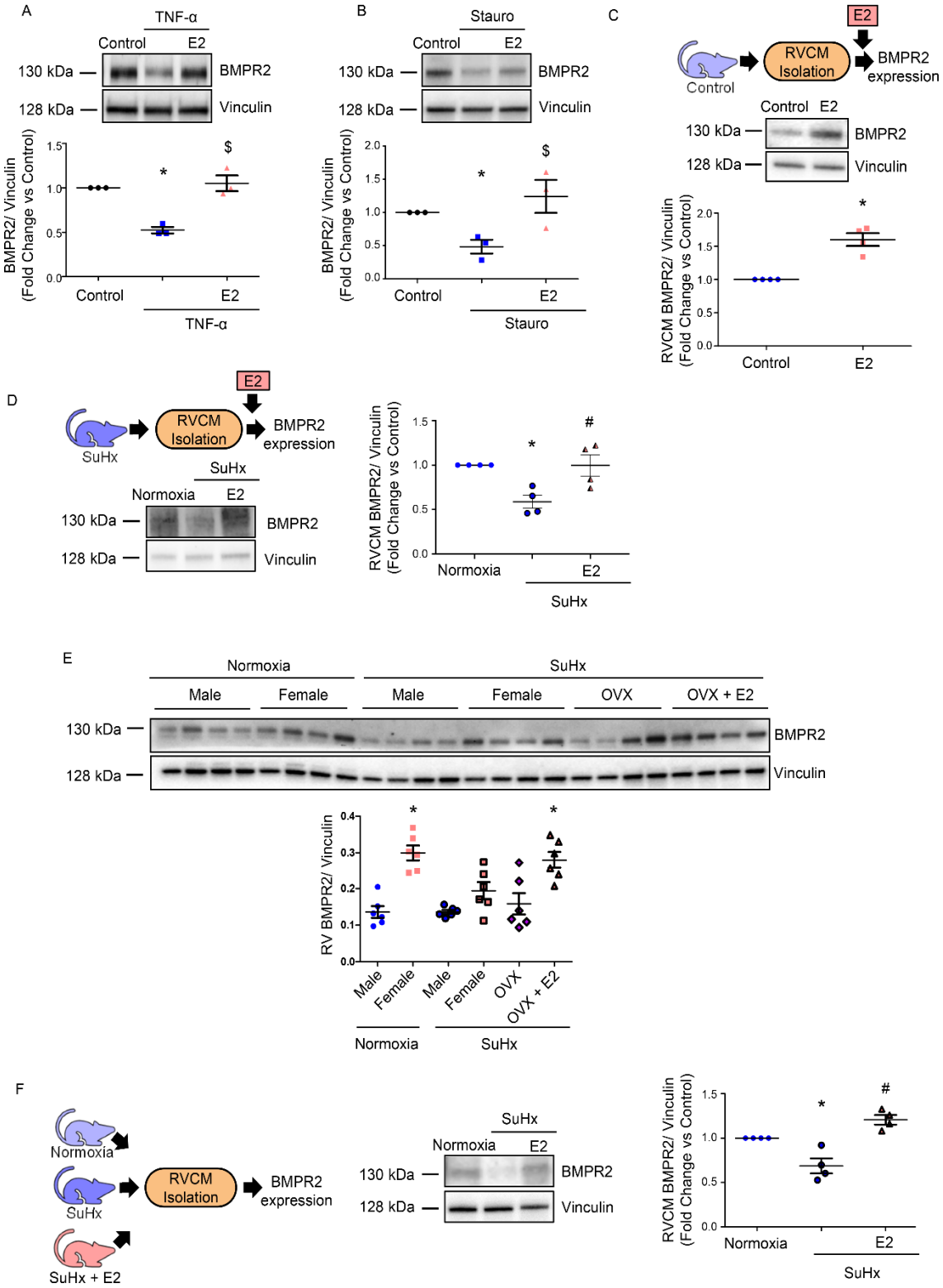
A
TNF-α
Control
E2
130 kDa
BMPR2
128 kDa
Vinculin
BMPR2/ Vinculin (Fold Change vs Control)
Control
E2
TNF-α
B
Stauro
Stauro
C
E2
RVCM Isolation
BMPR2 expression
Control
RVCM BMPR2/ Vinculin (Fold Change vs Control)
D
SuHx
Normoxia
E
Male
Female
OVX
OVX + E2
RV BMPR2/ Vinculin
F
Normoxia
SuHx
SuHx + E2

Figure 9. E2 upregulates BMPR2 in stressed cardiomyoblasts, in SuHx-PH RVs, and in RV cardiomyocytes (RVCMs). (**A, B**) Effects of E2 on BMPR2 expression in H9c2 cardiomyoblasts treated with TNF-α (10 ng/ml, 8h; **A**) or staurosporine (stauro; 50 nM, 4h; **B**). Cells were pretreated with E2 (100 nM) for 24h prior to TNF/stauro exposure and then lysed and analyzed by Western blot. (**C**) Western blot of BMPR2 expression in RVCMs isolated from male control rats treated with E2 in vitro (10 nM, 24h). (**D**) Western blot of BMPR2 expression in RVCMs isolated from male and female SuHx-PH rats and treated in vitro with E2 (10 nM, 24h). (**E**) Effects of endogenous or exogenous E2 on RV BMPR2 expression. SuHx-PH was induced in male, intact female, and ovariectomized (OVX) female rats. A subgroup of OVX females was replete with E2 (75 μg/kg/day via subcutaneous pellets for 7 weeks). Note higher baseline BMPR2 expression in female controls compared to males and increased RV BMPR2 protein abundance after E2 treatment. (**F**) BMPR2 expression evaluated by Western blot in RVCMs isolated from male normoxic control rats, untreated SuHx-PH rats, and SuHx-PH rats treated with E2 (75 μg/kg/day; subcutaneous pellets) for 7 weeks. N=3 independent experiments in (A&B); cells isolated from N=4 rats/group in (C, D, F), with each data point indicating one animal; N=6 rats/group in (E). Figures depict representative Western blots with densitometric analyses for all experiments. *$p<0.05$ vs. untreated control, $^{\$}p<0.05$ vs. TNF or stauro treatment in (A&B); *$p<0.05$ vs. untreated control in (C); *$p<0.05$ vs. normoxia control, $^{\#}p<0.05$ vs. untreated SuHx in (D,&F). *$p<0.05$ vs. male normoxic control in (E). All p-values by ANOVA with post-hoc Tukey correction except for (C), where p-value is by Student's t-test. Error bars represent means ± SEM; each data point represents one experiment or animal.

Figure 10.

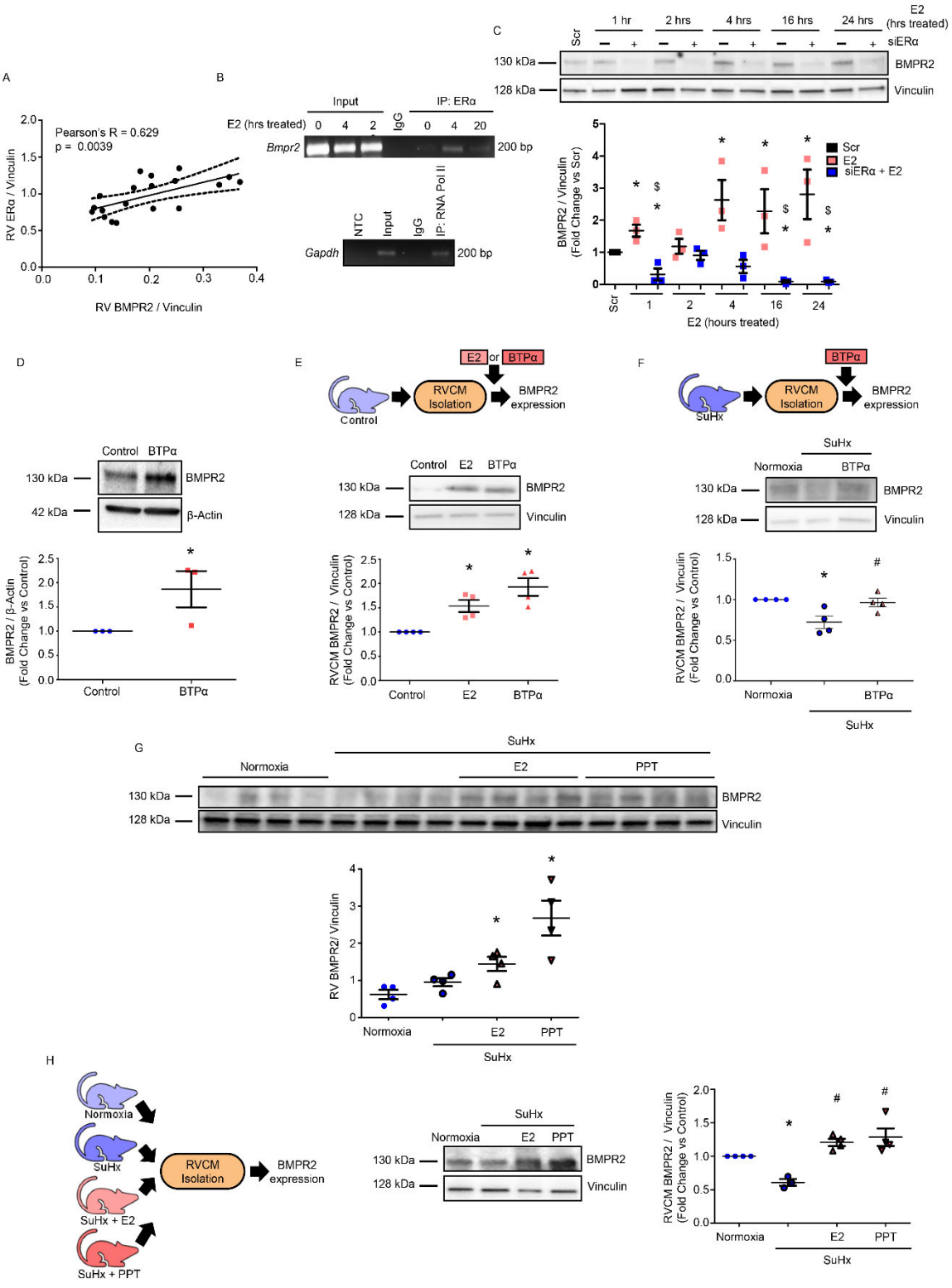
A
Pearson's R = 0.629
p = 0.0039
RV ERα / Vinculin
RV BMPR2 / Vinculin
B
Input
IP: ERα
E2 (hrs treated) 0 4 2 IgG 0 4 20
Bmpr2
200 bp
NTC
Input
IgG
IP: RNA Pol II
Gapdh
200 bp
C
1 hr
2 hrs
4 hrs
16 hrs
24 hrs
E2 (hrs treated)
Scr
siERα
130 kDa
BMPR2
128 kDa
Vinculin
BMPR2 / Vinculin (Fold Change vs Scr)
Scr
E2
siERα + E2
E2 (hours treated)
D
Control BTPα
130 kDa
BMPR2
42 kDa
β-Actin
BMPR2 / β-Actin (Fold Change vs Control)
Control
BTPα
E
E2 or BTPα
Control
RVCM Isolation
BMPR2 expression
Control E2 BTPα
130 kDa
BMPR2
128 kDa
Vinculin
RVCM BMPR2 / Vinculin (Fold Change vs Control)
Control
E2
BTPα
F
BTPα
SuHx
RVCM Isolation
BMPR2 expression
SuHx
Normoxia BTPα
130 kDa
BMPR2
128 kDa
Vinculin
RVCM BMPR2 / Vinculin (Fold Change vs Control)
Normoxia
BTPα
SuHx
G
SuHx
Normoxia
E2
PPT
130 kDa
BMPR2
128 kDa
Vinculin
RV BMPR2/ Vinculin
Normoxia
E2
PPT
SuHx
H
Normoxia
SuHx
SuHx + E2
SuHx + PPT
RVCM Isolation
BMPR2 expression
SuHx
Normoxia E2 PPT
130 kDa
BMPR2
128 kDa
Vinculin
RVCM BMPR2 / Vinculin (Fold Change vs Control)
Normoxia
E2
PPT
SuHx

Figure 10. ERα binds to *Bmpr2* promoter and is necessary and sufficient to increase RV BMPR2 in vitro and in vivo. (**A**) RV BMPR2 and ERα protein correlate positively in male and female control and SuHx-PH rats. (**B**) Chromatin immunoprecipitation of ERα binding at the *Bmpr2* promoter. H9c2 cardiomyoblasts were treated with E2 (100 nM) for 0 (control), 4 or 20h. DNA/protein complexes were cross-linked and immunoprecipitated with anti-ERα antibody or IgG isotype control. RNA Polymerase II (RNA Pol II) binding to *Gapdh* promoter was used as positive control (bottom panel). NTC=no template control. (**C**) Time-course of BMPR2 expression in H9c2 cardiomyoblasts after ERα siRNA knockdown (5 nM; 24h prior to E2 [100 nM]; see Fig. 4B for ERα knockdown efficacy). (**D**) BMPR2 protein in H9c2 cells treated with ERα-agonist BTPα (100 nM, 24h). (**E**) BMPR2 protein in RV cardiomyocytes (RVCMs) isolated from male rats and treated with E2 (10 nM, 24h) or BTPα (100 nM, 24h) in vitro. (**F**) BMPR2 protein in RVCMs isolated from male and female SuHx-PH rats and treated in vitro with BTPα (100 nM, 24h). (**G**) BMPR2 expression in RV homogenates from male normoxia, SuHx-PH, or SuHx-PH rats treated with E2 or ERα-agonist PPT (75 or 850 μg/kg/day; subcutaneous pellets). (**H**) BMPR2 protein in RVCMs from groups shown in (F). N=3 independent experiments in (B-D); N=4 rats/group in (E-H). (B-G) depict representative Western blots. Densitometries include data from all experiments or animals. Pearson's R-value and p-value shown in (A). Dashed lines represent 95%-confidence intervals. *p<0.05 vs. Scr (scrambled control), $^{\$}$p<0.05 vs. E2 in (C); *p<0.05 vs. control or normoxia in (D-H); $^{\#}$p<0.05 vs. untreated SuHx in (F&H). P-values in (B&C, E-H) by ANOVA/post-hoc Tukey correction; p-value in (D) by Student's t-test. Error bars represent means ± SEM; each data point represents one experiment/animal.

1076 **Figure 11.**

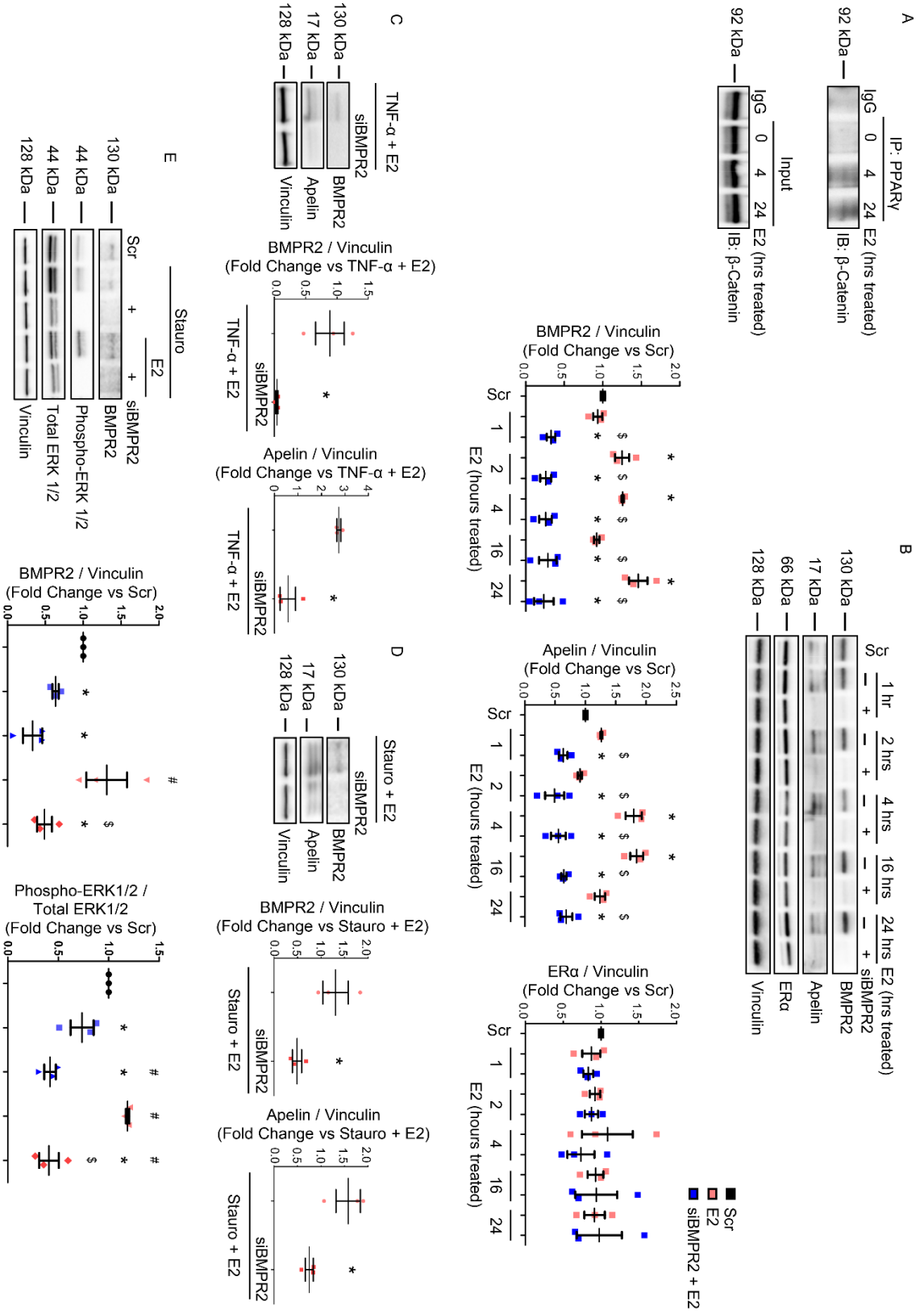

1077

Figure 11. E2 induces formation of PPAR/-catenin complexes and requires BMPR2 to increase apelin expression or ERK1/2 activation in cardiomyoblasts. (**A**) H9c2 cardiomyoblasts were treated with E2 (100 nM) for 0, 4 or 24h and then immunoprecipitated with PPARγ antibody or rabbit IgG isotype control. Input control for each sample is indicated (bottom). Note formation of PPARγ/β-catenin complexes with E2 treatment at 4 and 24h. (**B**) Time course of siRNA knockdown of BMPR2 (5 nM) effects on apelin protein expression in E2-treated (100 nM) H9c2 rat cardiomyblasts at baseline conditions. (**C, D**) Effects of BMPR2 knockdown on E2-mediated upregulation of apelin in stressed cardiomyoblasts. H9c2 cells were pretreated with E2 (100 nM, 24h) and then stressed with TNF-α (10 ng/ml, 8h; **C**) or staurosporine (stauro; 50 nM, 4h; **D**) ± siRNA knockdown of BMPR2 (5 nM, 24h prior to E2). (**E**) Effects of BMPR2 knockdown on E2-mediated ERK1/2 activation in stressed cardiomyoblasts. Cells were pretreated with E2 (100 nM, 24h) and then treated with staurosporine (stauro; 50 nM, 4h) ± siRNA directed against BMPR2 (5 nM; 24h prior to E2 and stauro). Representative blots for three independent experiments shown in (A, B-E). Densitometries include data from all experiments. Scr = scramble siRNA. *p<0.05 vs. Scr control, $^{\$}$p<0.05 vs. E2 by ANOVA with post-hoc Tukey's correction in (B); *p<0.05 vs. TNF + E2 or Stauro + E2 by Student's t-test in (C, D); *p<0.05 vs. Scr control, $^{\#}$p<0.05 vs. Stauro, $^{\$}$p<0.05 vs. E2-treated Stauro group by ANOVA with post-hoc Dunnett's correction in (E). Error bars represent means ± SEM; each data point represents one experiment or animal.

Figure 12.

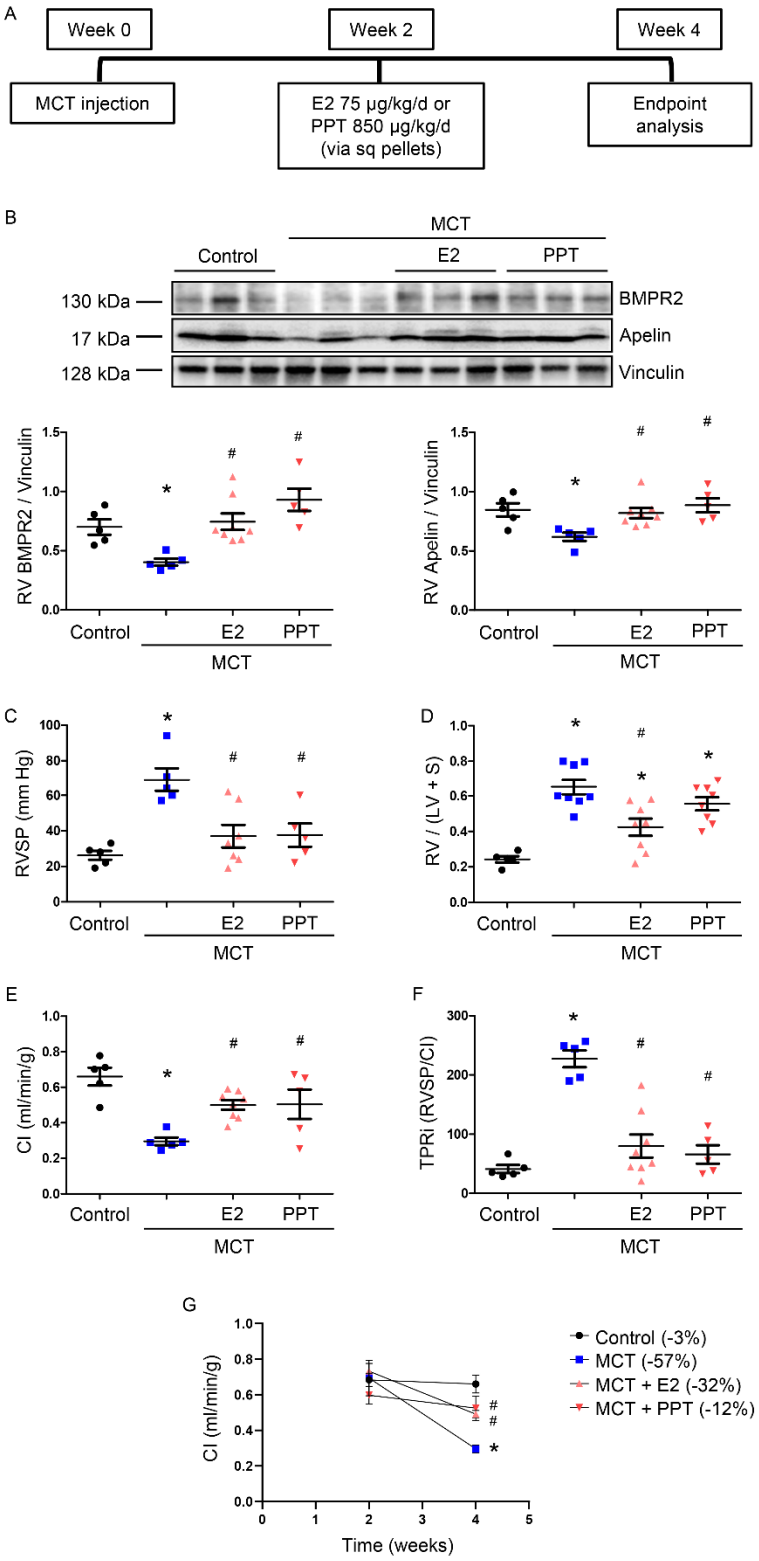
A
Week 0
Week 2
Week 4
MCT injection
E2 75 µg/kg/d or PPT 850 µg/kg/d (via sq pellets)
Endpoint analysis
B
MCT
Control
E2
PPT
130 kDa
17 kDa
128 kDa
BMPR2
Apelin
Vinculin
RV BMPR2 / Vinculin
RV Apelin / Vinculin
C
RVSP (mm Hg)
D
RV / (LV + S)
E
CI (ml/min/g)
F
TPRi (RVSP/CI)
G
CI (ml/min/g)
Time (weeks)
Control (-3%)
MCT (-57%)
MCT + E2 (-32%)
MCT + PPT (-12%)

Figure 12. E2 or ERα agonist PPT rescues monocrotaline (MCT)-induced PH and increases RV BMPR2 and apelin. (**A**) Experimental design. (**B**) Western blot analysis of RVs from MCT-PH rats. A representative Western blot is depicted on top of the panel; densitometric analysis from all experimental animals is shown at bottom. (**C-F**) Effects of E2 or PPT on RV systolic pressure (RVSP; **C**), RV hypertrophy (RV weight divided by weight of left ventricle plus septum; RV / [LV+S]; **D**), cardiac index (echocardiographic cardiac output / body weight; **E**), and total pulmonary resistance index (cardiac index / RVSP; **F**). (**G**) Time-course of CI. Percent change in CI vs 2-week baseline time point is shown in legend in parentheses behind group names. *$p<0.05$ vs control, $^{\#}p<0.05$ vs. untreated MCT (one-way ANOVA with Tukey or Dunnett's post-hoc correction). Each data point in (B-F) represents one male animal. Error bars represent means ± SEM. Sq = subcutaneous.

Figure 13.

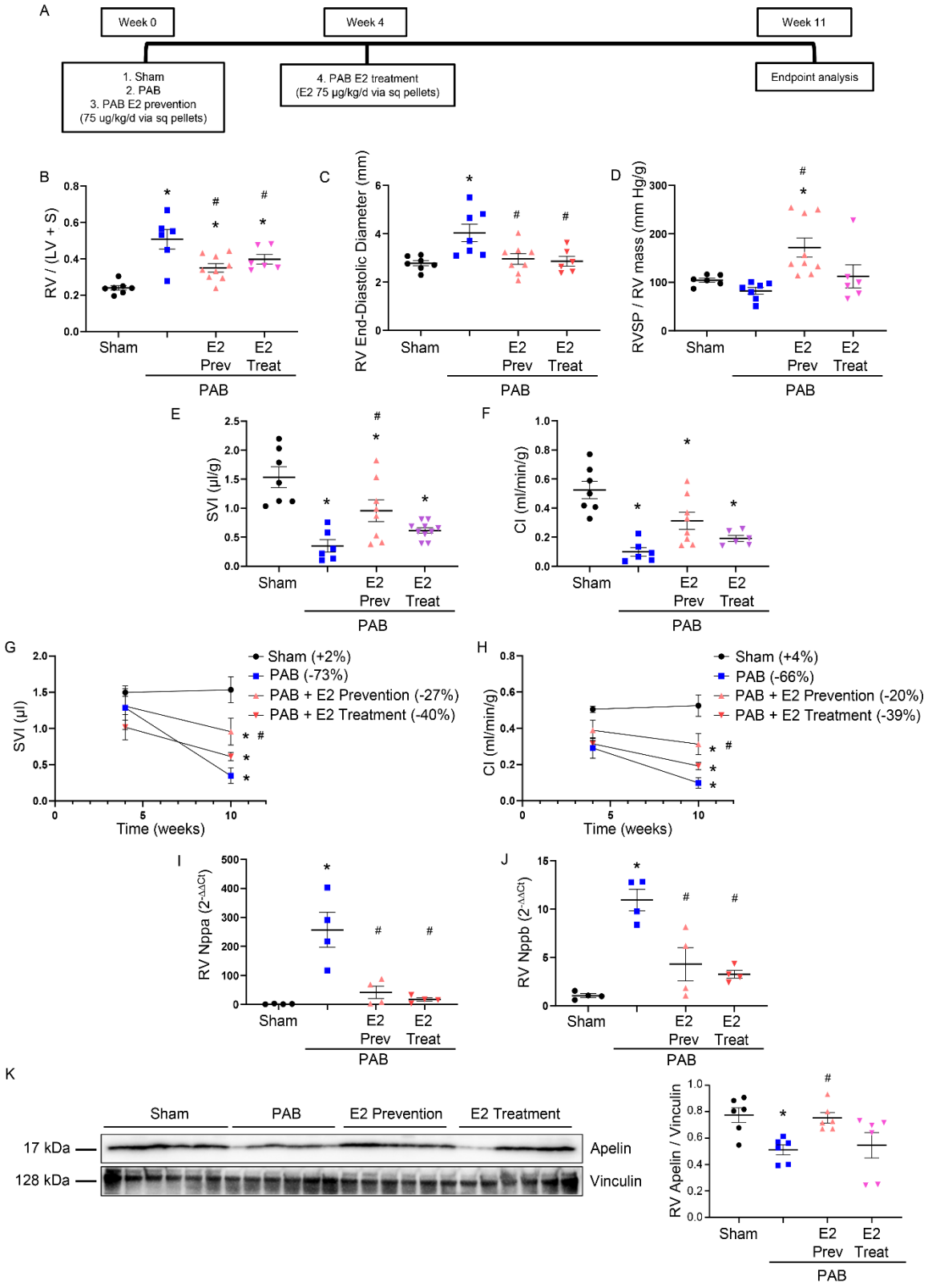
A
Week 0
Week 4
Week 11
1. Sham
2. PAB
3. PAB E2 prevention
(75 ug/kg/d via sq pellets)
4. PAB E2 treatment
(E2 75 µg/kg/d via sq pellets)
Endpoint analysis
B
RV / (LV + S)
C
RV End-Diastolic Diameter (mm)
D
RVSP / RV mass (mm Hg/g)
E
SVI (µl/g)
F
CI (ml/min/g)
Sham
E2 Prev
E2 Treat
PAB
G
SVI (µl)
Sham (+2%)
PAB (-73%)
PAB + E2 Prevention (-27%)
PAB + E2 Treatment (-40%)
Time (weeks)
H
CI (ml/min/g)
Sham (+4%)
PAB (-66%)
PAB + E2 Prevention (-20%)
PAB + E2 Treatment (-39%)
Time (weeks)
I
RV Nppa (2-ΔΔCt)
J
RV Nppb (2-ΔΔCt)
K
Sham
PAB
E2 Prevention
E2 Treatment
17 kDa
128 kDa
Apelin
Vinculin
RV Apelin / Vinculin

Figure 13. E2 prevents and rescues RV failure induced by pulmonary artery banding (PAB). (**A**) Experimental design. (**B-H**) Effects of E2 treatment on RV hypertrophy (RV weight divided by weight of left ventricle plus septum; RV / [LV+S]; **B**), RV end-diastolic diameter (**C**), RV systolic pressure (RVSP) normalized for RV mass (**D**), stroke volume index (SVI; **E**) and cardiac index (**F**). SVI and CI were determined echocardiographically. (**G-H**) Time-courses of SVI and CI. Percent change in SVI and CI vs 4-week baseline time point is shown in legends in parentheses behind group names. (**I-J**) Effects of E2 treatment on atrial natriuretic peptide (Nppa, **I**) and B-type natriuretic peptide (Nppb, **J**) by real time RT-PCR. (**K**) Quantification of RV apelin by Western blot and densitometric analysis. *$p<0.05$ vs sham control, $^{\#}p<0.05$ vs untreated PAB (one-way ANOVA with Tukey or Dunnett's post-hoc correction). Each data point in (B-F, I-K) represents one male animal. Error bars represent means ± SEM. Sq = subcutaneous; Prev = prevention group; Treat = treatment group.